

Copyright
by
Thomas G. Etienne
2018

THE LAMB SHIFT AT FINITE TEMPERATURE AND DENSITY

by

Thomas G. Etienne, B.S.

THESIS

Presented to the Faculty of
The University of Houston-Clear Lake
In Partial Fulfillment
Of the Requirements
For the Degree

MASTER OF SCIENCE

in Physics

THE UNIVERSITY OF HOUSTON-CLEAR LAKE

MAY, 2018

THE LAMB SHIFT AT FINITE TEMPERATURE AND DENSITY

by

Thomas G. Etienne

APPROVED BY

Samina S. Masood, Ph.D., Chair

Van E. Mayes, Ph.D., Committee Member

Ju H. Kim, Ph.D., Committee Member

APPROVED/RECEIVED BY THE COLLEGE OF SCIENCE AND ENGINEERING:

Said Bettayeb, Ph.D., Associate Dean

Ju H. Kim, Ph.D., Dean

Acknowledgements

I would like to express my sincerest appreciation to my committee chair, Dr. Samina Masood, who has accommodated my high school teaching job by dedicating her weekends and after evenings to helping me better understand the denotation of complexity that is quantum field theory. Not only was she willing donate her time over college breaks, but she insisted upon it, understanding that these were the times that best suited me. She took me under her wing since my first graduate class in Astroparticle Physics, and continuously checked in with me to make certain that I stay on track throughout my Master's program. With my busy lifestyle, I can at least say it would have taken me longer to graduate without her guidance. Working with her was an inspiration and a constant reminder of what it means to be a good teacher.

I would like to thank my committee members Dr. Van E. Mayes and Dr. Ju H. Kim for dedicating their time to my thesis. I am forever grateful that they were able to find the time to provide edits and insight to the development of my thesis amidst their busy schedules.

I would like to thank my parents, Christine and Greg Etienne, for their incessant love and support throughout my time in Houston. Though they may never read this thesis, I hope they are honored by it, as I can easily say I could not have done it without them. I would like to thank the rest of my family and friends from back home in Michigan and everywhere else for their support, especially those who visited me during my time here in Houston to ensure that I maintain my sanity. Likewise, a special thanks is also given to my new friends that I have made here in Houston. Lastly, I would like to thank my students whose support and respect has provided me with enough motivation to keep pushing forward. I started graduate school 3 years ago in hopes that I would always be able to provide concrete answers to their inquisitive questions. Thank you.

ABSTRACT

THE LAMB SHIFT AT FINITE TEMPERATURE AND DENSITY

Thomas G. Etienne
University of Houston-Clear Lake, 2018

Thesis Chair: Samina S. Masood, Ph.D.

The Lamb shift is a well-known phenomenon that breaks the degeneracy in the $2S_{1/2}$ and $2P_{1/2}$ energy levels. The currently accepted experimental value is measured to be approximately equal to 1057.862 MHz, or 4.3795×10^{-6} eV, and theoretically calculated values are very close to this. Theoretical derivation requires a perturbative approach of quantum field theory. Renormalization constants of Quantum Electrodynamics (QED) such as vacuum polarization, self-energy, and radiative corrections to the wave function of the electron contribute to the currently accepted theoretical value of the Lamb shift. We review the structure of the hydrogen atom and the Lamb shift of its $2S_{1/2}$ and $2P_{1/2}$ energy levels in isolation, and then calculate the temperature and density contributions to the Lamb shift for extremely hot and dense media using the real time approach of QED, which give all the radiative corrections in the form of Masood's function in many body QED. This result has very important applications in astrophysics and cosmology.

TABLE OF CONTENTS

List of Figures	vii
Chapter	Page
CHAPTER I: INTRODUCTION.....	1
Equations of Motion	2
Schrödinger’s Hydrogen Atom.....	6
Relativistic Quantum Mechanics	10
Dirac Solution for Hydrogen Atom	13
CHAPTER II: QUANTUM FIELD THEORY.....	17
Perturbation Theory and the S-Matrix	17
The Propagator.....	21
Quantum Electrodynamics.....	26
Renormalization.....	34
CHAPTER III: RENORMALIZATION OF QED	39
Vacuum Polarization.....	40
Electron Self-Energy.....	47
Vertex Corrections and Anomalous Magnetic Moment	50
The Lamb Shift	55
CHAPTER IV: LAMB SHIFT AT FINITE TEMPERATURE	61
Blackbody Radiation Corrections to the Lamb Shift.....	62
Quantum Fluctuations and the Lamb Shift	66
Renormalization of QED at Finite Temperature and Density	71
Lamb Shift at Finite Temperature.....	76
Lamb Shift at Finite Chemical Potential.....	82
Discussion of Results and Extensions.....	83
REFERENCES	88

LIST OF FIGURES

Figure	Page
Figure 1.1 – Schrödinger’s Energy Levels	10
Figure 1.2 – Schrödinger, Dirac, and QED Energy Levels	16
Figure 2.2 – Feynman Diagrams for Fermions.....	31
Figure 2.3 – Additional Feynman Rules for QED	32
Figure 3.1 – Vacuum Polarization	40
Figure 3.2 – 1-Loop Correction to Fermion Propagator	48
Figure 3.3 – Vertex Correction	51
Figure 4.1 – Lamb Shift with Blackbody Radiation Corrections	65
Figure 4.2 – Lamb Shift due to Quantum Fluctuations	70
Figure 4.3 – Lamb Shift at Finite Temperature with QED Corrections ($T \ll m$).....	78
Figure 4.4 – Lamb Shift at Finite Temperature with QED Corrections ($T \gg m$).....	78
Figure 4.5 – Blackbody Mixing Corrections with QED Thermal Corrections.....	81
Figure 4.6 – Comparison of Blackbody Corrections and QED Blackbody Corrections ...	81
Figure 4.7 – Lamb Shift in High Chemical Potential	83

CHAPTER I: INTRODUCTION

Structure of the hydrogen atom is determined from solving Schrödinger's equation in quantum mechanics. However, the detailed study of structure includes a very small change in the energy levels of different orbitals. This cannot be explained without the use of relativistic contributions, which can be calculated using the perturbative techniques of quantum field theory. The Lamb shift is a small amount of energy that breaks degeneracy in the $2S_{1/2}$ and $2P_{1/2}$ energy levels; theoretically it is determined by radiative corrections. The currently accepted experimental value is measured to be approximately equal to 1057.862 MHz, or 4.38×10^{-6} eV, and theoretical calculations have come very close to this [2].

Calculation of the Lamb shift gives the precise measurement of the orbital energy of the hydrogen atom, which is needed to describe the correct structure of the atom. Calculation of the thermal contribution to the Lamb shift will help to determine the detailed structure of the hydrogen atom. The complexity of orbital structure of hydrogen, or any other atom, is revealed by the application of perturbative quantum mechanics. These techniques are used to calculate small changes in energy that are needed to break degeneracy and correctly understand the distribution of electron energy within the energy orbitals. At high energies, quantum mechanical approach is to be replaced by quantum field theory, and analytical techniques of perturbative quantum electrodynamics (QED) is applied to study the orbital distributions in a more accurate manner. Quantum statistical physics becomes increasingly more relevant when studying electrodynamic interactions in hot and dense media like stellar cores and the early universe. For this purpose, the real-time perturbation theory is used. In order to calculate finite temperature and density

(FTD) effects of QED on the Lamb shift, it is first necessary to understand how the Lamb shift is calculated in quantum mechanics, and then at higher energies in QED vacuum. In this chapter, the transition from classical mechanics to quantum mechanics is reviewed, and Schrödinger's solution to hydrogen structure is discussed. Discussion will then follow as to why quantum field theory is necessary to incorporate relativistic effects, allowing for real time analysis of perturbative effects.

Equations of Motion

The Euler-Lagrange equation of motion is considered to be the most general equation of motion and can be solved to describe the dynamics of the hydrogen atom. D'Alembert's principle, or calculus of variation, are common approaches to determining hydrogen structure [16]. The most basic definition from Newton's laws for the classical trajectory of a particle in a conservative potential is given by

$$m\ddot{x} = -\frac{dV}{dx} \quad [1.1.1]$$

It might not be as obvious in classical mechanics as to why the above equation needs to be reformulated, but it should be relatively obvious from a quantum mechanical standpoint: seeing as how this equation gives the impression that we would be able to find an equation for the position of a particle in a well-defined potential. Obviously this is not realistic in the realm of quantum mechanics, so we will now take steps to find equations of motion purely in terms of energies, which are measurable quantities.

In dealing primarily with the single electron hydrogen atom, we will be treating our electron-proton system as a central force orbital problem, where the total energy will remain a constant, so that $E = T + V$, where T is the kinetic energy and V is the potential

energy. We may write the average kinetic energy and average potential energy respectively as

$$\bar{T} = \frac{1}{\tau} \int_0^\tau \frac{1}{2} m [\dot{x}(t)]^2 dt \quad \text{and} \quad \bar{V} = \frac{1}{\tau} \int_0^\tau V [x(t)] dt \quad [1.1.2]$$

This problem needs to be generalized to many different independent variables, thus it is necessary to use the techniques of the calculus of variations, otherwise known as Hamilton's principle [1, 16]. It can be shown that the average kinetic and average potential energies vary from their classical trajectories like

$$\frac{\delta \bar{V}(x)}{\delta x(t)} = \frac{V'(x)}{\tau} \quad \text{and} \quad \frac{\delta \bar{T}(x)}{\delta x(t)} = \frac{-m\ddot{x}}{\tau} \quad [1.1.3]$$

With a substitution of equation (1.1.1) into the equation on the left in (1.1.3), the average kinetic and average potential energies are related through the equation

$$\frac{\delta}{\delta x(t)} [\bar{T}(x) - \bar{V}(x)] = 0 \quad [1.1.4]$$

Equation (1.1.4) implies that the difference between the average kinetic energy and the average potential energy is stationary around the classical trajectory of a system. This provides motivation to define a Lagrangian L as $L = T - V$. The action S will be defined as the integral of the Lagrangian over time, so that $S = \int_0^\tau L dt$, and the units for action are conveniently shared with that of Planck's constant h . Hamilton's principle states that the trajectory a particle will take can be determined from the condition of least action such that the rate of change of action vanishes:

$$\frac{\delta S}{\delta x(t)} = 0 \quad [1.1.5]$$

A substitution of the definition of the action as the integral involving the Lagrangian, and following an application of the Leibniz integral rule, the Euler-Lagrange equation in generalized coordinates is

$$\frac{\partial L}{\partial q_i} - \frac{d}{dt} \frac{\partial L}{\partial \dot{q}_i} = 0 \quad [1.1.6]$$

For a Lagrangian $L(q_i, \dot{q}_i, t)$, we can write

$$dL = \frac{\partial L}{\partial q_i} dq_i + \frac{\partial L}{\partial \dot{q}_i} d\dot{q}_i + \frac{\partial L}{\partial t} dt \quad [1.1.7]$$

With substitutions for the canonical momentum $p_i = \partial L / \partial \dot{q}_i$ and the time derivative for the canonical momentum $\dot{p}_i = \partial L / \partial q_i$, a Legendre transformation is used to arrive at the Hamiltonian H written in terms of the Lagrangian as

$$H = p_i \dot{q}_i - L \quad [1.1.8]$$

The Hamiltonian is simply equal to the total energy so long as the potential is derived from a conservative force, and the equations defining the generalized coordinates don't depend on time. In looking at variations in the Hamiltonian, we will eventually determine the first-order equations of motion known as Hamilton's equations

$$\dot{q}_i = \frac{\partial H}{\partial p_i} \quad \text{and} \quad -\dot{p}_i = \frac{\partial H}{\partial q_i} \quad [1.1.9]$$

It is shown classically [1, 16] how naturally Lagrangians and Hamiltonians for continuous systems may be transformed into Lorentz covariant actions by defining the Lagrange \mathcal{L} and Hamiltonian \mathcal{H} densities.

$$L = \int d^3x \mathcal{L} \quad \text{and} \quad H = \int d^3x \mathcal{H} \quad [1.1.10]$$

The Lagrange and Hamiltonian densities will prove to be more useful for relativistic treatment. The relationship between the Hamiltonian density and the Lagrangian density can now be written as

$$\mathcal{H} = \Pi \dot{\phi} - \mathcal{L} \quad [1.1.11]$$

where $\Pi(x) = \frac{\partial \mathcal{L}}{\partial \dot{\phi}}$ is the conjugate momentum, and ϕ is the field component which will be defined in more detail later on. Equation (1.1.6) will also transform nicely to

$$\frac{\partial \mathcal{L}}{\partial \phi} - \partial_\mu \left(\frac{\partial \mathcal{L}}{\partial (\partial_\mu \phi)} \right) = 0 \quad [1.1.12]$$

The rate of change of any general function F can be written as

$$\frac{dF}{dt} = \frac{\partial F}{\partial t} + \frac{\partial F}{\partial q_i} \dot{q}_i + \frac{\partial F}{\partial p_i} \dot{p}_i = \frac{\partial F}{\partial t} + \{F, H\} \quad [1.1.13]$$

The final term in equation (1.1.13) is the Poisson bracket with the Hamiltonian. If the function F does not depend explicitly on time, then the Poisson bracket will be equal to zero, and the function F is a constant of the motion. By looking at the rate of change of the expectation value of an operator \hat{F} , we can relate any Poisson bracket to the commutator in quantum mechanics [1] by

$$\{F, H\} \rightarrow \frac{1}{i\hbar} \langle [\hat{F}, \hat{H}] \rangle \quad [1.1.14]$$

Up to this point, we have really only reviewed some of the main formalisms of classical mechanics, while hinting at some transitions that need to be made to incorporate relativistic quantum mechanics. The purpose of this section was to show that it is possible to describe complex systems in terms of Lagrangian and Hamiltonians through the aforementioned equations. In the next section, a transition will be made to the realm of quantum mechanics; keeping in mind, that we may also transition to relativistic formulation by transforming our Lagrangian and Hamiltonians to Lagrangian densities and Hamiltonian densities, respectively.

Schrödinger's Hydrogen Atom

The study of the hydrogen atom is one of the more popular topics in quantum mechanics, particularly because it is a two-body problem. In quantum mechanics, the energy $\hat{E} = i\hbar \frac{\partial}{\partial t}$ and momentum $\hat{p} = -i\hbar\nabla$ are operators that act on the wave function $\psi(\vec{x}, t)$. For systems in which the total energy is given by the Hamiltonian [4],

$$\hat{E}\psi(\vec{x}, t) = \hat{H}\psi(\vec{x}, t) \quad [1.2.1]$$

For the free-particle, it can be easily seen that the wave function has plane-wave solutions of the form $\psi(\vec{x}, t) = Ne^{-i(\omega t - \vec{k} \cdot \vec{x})}$. From the plane-wave solution, it is also clear that the eigenvalues are $\hbar k$ for the momentum operator, and $\hbar\omega$ for the energy operator.

For the single electron hydrogen atom, a potential is included, so that the Hamiltonian is given by

$$\hat{H} = -\frac{\hbar^2}{2\mu}\nabla^2 + V(r) \quad [1.2.2]$$

where μ is the reduced mass $\mu = \frac{m_e m_p}{m_e + m_p}$, and $V(r)$ is the potential energy, which is assumed to depend only on the radial separation of the proton and electron. Rewriting the kinetic energy term of the Hamiltonian in spherical polar coordinates, and making a substitution with the angular momentum operator

$$\hat{L}^2 = -\hbar^2 \left[\frac{1}{\sin\theta} \frac{\partial}{\partial\theta} \left(\sin\theta \frac{\partial}{\partial\theta} \right) + \frac{1}{\sin^2\theta} \frac{\partial^2}{\partial\theta^2} \right] \quad [1.2.3]$$

equation (1.2.2) is written as

$$\left\{ -\frac{\hbar^2}{2\mu} \left[\frac{1}{r^2} \frac{\partial}{\partial r} \left(r^2 \frac{\partial}{\partial r} \right) - \frac{\hat{L}^2}{\hbar^2 r^2} \right] + V(r) \right\} \psi(\vec{r}) = E\psi(\vec{r}) \quad [1.2.4]$$

The potential energy term will be written as $V(r) = -\frac{Ze^2}{(4\pi\epsilon_0)r}$ which may be general for any single-electron atom with a nucleus of charge Ze , and r is the distance between the electron and the nucleus. Since the primary focus here is on the hydrogen atom, Z will be taken to be equal to 1. The wave function in equation (1.2.4) is then written in terms of a radial function and the spherical harmonics [4]. It is already known that the spherical harmonics are eigenfunctions of the angular momentum operator, and are given as

$$\hat{L}^2 Y_{lm}(\theta, \phi) = l(l+1)\hbar^2 Y_{lm}(\theta, \phi) \quad [1.2.5]$$

With these substitutions, equation (1.2.4) is now written in terms of just the radial wave function $R_{El}(r)$ as

$$\left[-\frac{\hbar^2}{2\mu} \left(\frac{d^2}{dr^2} + \frac{2}{r} \frac{d}{dr} \right) + \frac{l(l+1)\hbar^2}{2\mu r^2} - \frac{Ze^2}{(4\pi\epsilon_0)r} \right] R_{El}(r) = ER_{El}(r) \quad [1.2.6]$$

The final two terms in the brackets may also look familiar from studies involving orbital mechanics, where the angular momentum term may be thought of as a centrifugal barrier. In this way, these final two terms can be combined into an effective potential such that

$$V_{eff}(r) = \frac{l(l+1)\hbar^2}{2\mu r^2} - \frac{Ze^2}{(4\pi\epsilon_0)r} \quad [1.2.7]$$

Solutions for equation (1.2.6) then begin with a substitution for some radial function $u_{El}(r) = rR_{El}(r)$ [4]. The Schrödinger equation then reduces to

$$\frac{d^2 u_{El}(r)}{dr^2} + \frac{2\mu}{\hbar^2} [E - V_{eff}(r)] u_{El}(r) = 0 \quad [1.2.8]$$

We will be focusing our attention on situations for $E < 0$, where bound states may exist within the effective potential. It is also convenient to develop dimensionless quantities $\rho = \left(-\frac{8\mu E}{\hbar^2}\right)^{1/2} r$ and $\lambda = Z\alpha \left(-\frac{\mu c^2}{2E}\right)^{1/2}$, where $\alpha = e^2/(4\pi\epsilon_0\hbar c) \approx \frac{1}{137}$ is

the fine structure constant [4]. With substitutions of these dimensionless quantities into equation (1.2.8), the equation to be solved is written as

$$\left[\frac{d^2}{d\rho^2} - \frac{l(l+1)}{\rho^2} + \frac{\lambda}{\rho} - \frac{1}{4} \right] u_{El}(\rho) = 0 \quad [1.2.9]$$

It is noted that when ρ approaches infinity, the middle two terms in the brackets of equation (1.2.9) become negligible, so that for large ρ , solutions to the above equation are exponential functions. Since the initial assumption was that $E < 0$, primary focus is on the bound states so that exponential functions that vanish at infinity will be kept. The radial equation should then have solutions like $u_{El}(\rho) = e^{-\rho/2} f_{El}(\rho)$ [4]. Substitution of this expression into equation (1.2.9) then gives

$$\left[\frac{d^2}{d\rho^2} - \frac{d}{d\rho} - \frac{l(l+1)}{\rho^2} + \frac{\lambda}{\rho} \right] f_{El}(\rho) = 0 \quad [1.2.10]$$

An expansion of solution for $f(\rho)$ around the origin is made so that $f(\rho)$ can be written like $f(\rho) = \rho^{l+1} \sum_{k=0}^{\infty} c_k \rho^k$ where c_0 is not zero, and the assumption is made so that the function $f(\rho)$ behaves like ρ^{l+1} around the origin. Upon substituting this expansion into equation (1.2.10), a summation over the all values of k gives

$$\sum_{k=0}^{\infty} [[k(k+1) + (2l+2)(k+1)]c_{k+1} + (\lambda - l - 1 - k)c_k] \rho^k = 0 \quad [1.2.11]$$

Since the term in brackets of equation (1.2.11) must vanish separately from ρ^k , then the coefficients c_{k+1} and c_k are related by

$$c_{k+1} = \frac{k+l+1-\lambda}{(k+1)(k+2l+2)} c_k \quad [1.2.12]$$

To ensure that only radial functions with acceptable behavior are kept, it will be assumed that the series expansion terminates eventually at some value of $k = n_r$, where n_r

is the positive integer that is defined as the radial quantum number. Since this is the largest value of k allowed, it can be seen that $c_{n+1} = 0$. Then from equation (1.2.12) it is determined that $\lambda = n_r + l + 1$. The principle quantum number n is defined as $n = n_r + l + 1$ ($n = 1, 2, 3, \dots$). The eigenvalues for equation (1.2.9) are therefore $\lambda = n$. From the initial definition of λ , it is seen that the bound-state energy eigenvalues are discrete in nature, and Schrödinger's solution for the hydrogen atom energy levels yields

$$E_n = -\frac{1}{2} \mu c^2 \frac{\alpha^2}{n^2} = \frac{-13.6 \text{ eV}}{n^2} \quad n = 1, 2, 3, \dots \quad [1.2.13]$$

It is noted that the energy eigenvalues seen here depend only on the principle quantum number n , so that we have degeneracy with respect to the orbital and magnetic quantum numbers l and m . For each value of n , the orbital angular momentum quantum number is $n-1$ fold degenerate, and for each value of l , the magnetic quantum number m is $(2l + 1)$ fold degenerate. The total degeneracy can then be shown to be $2n^2$ when taking spin into account. The energy levels are shown in Figure 1.1 on the following page.

It will be shown in later sections that relativistic effects perturb these energy levels and break the degeneracy between the states. However, before doing this, a discussion will be given as to why quantum mechanics is no longer a viable approach if these effects are expected to be considered.

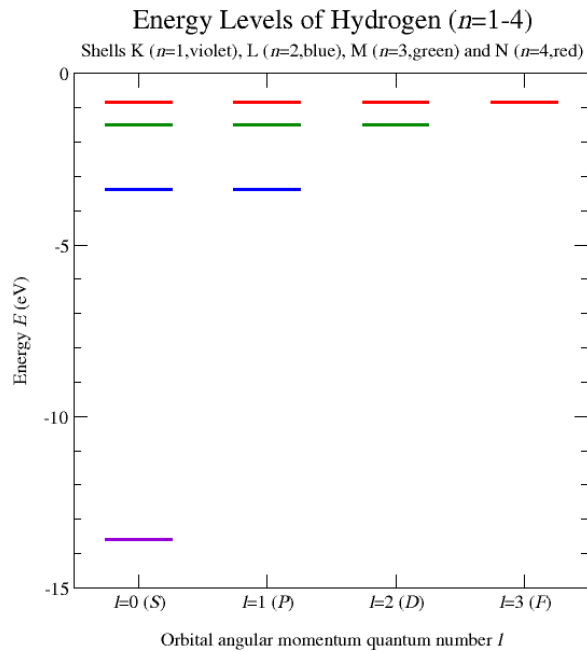


Figure 1.1 – Schrödinger’s Energy Levels

The energy levels of Hydrogen as determined by solving the Schrödinger equation with non-relativistic schemes.

https://commons.wikimedia.org/wiki/File:Hydrogen_energy_levels.png

Relativistic Quantum Mechanics

The Schrödinger picture in quantum mechanics is a representation that deals with time-independent operators and time-dependent state vectors. Stationary states of particles are associated with time independent wave functions. In the Heisenberg picture, the time evolution of a stationary state of particles is determined through time dependent operators. Conceptual significance of the Schrödinger representation is based on the fact that it allows for the annihilation of a state vector, which can then be once again created at a different instant in time. However, transition to such a representation brings up an unacceptable result: the probability amplitude for a single particle to exist beyond its forward light-cone is nonzero [1]. It is therefore not possible to reconcile special

relativity with single-particle quantum mechanics. In order to incorporate the relativistic effects properly, a transition is made from a single-particle notion to a quantized field notion.

The Klein-Gordon wave equation was the first attempt in constructing a relativistic formulation of quantum mechanics. The Einstein energy-momentum relationship $E^2 = m^2 + p^2$ in the natural units ($c = 1$) can be written in terms of the previously defined operators. This leads to the Klein-Gordon equation [9]

$$\frac{\partial^2 \psi}{\partial t^2} = \nabla^2 \psi - m^2 \psi \quad [1.3.1]$$

It is worth noting here that this equation gives a plane wave solution for the field, and more importantly, the speed at which the plane waves propagate for a massless particle would be the speed of light. It is common to express the Klein-Gordon equation in the Lorentz invariant form as

$$(\partial^\mu \partial_\mu + m^2)\psi = 0 \quad \partial^\mu \partial_\mu = \frac{\partial^2}{\partial t^2} - \frac{\partial^2}{\partial x^2} - \frac{\partial^2}{\partial y^2} - \frac{\partial^2}{\partial z^2} \quad [1.3.2]$$

As was mentioned above, the Klein-Gordon equation perfectly works for bosons and can be useful for the description of photons as massless particles. However, for massive particles, the solutions for the field from equations (1.3.1) and (1.3.2) give negative energy solutions described by unphysical negative probability densities [9].

The physical implications of the Klein-Gordon equation led Dirac to search for an alternative form of the first order wave equation to incorporate the half integral spin of particles. Dirac begins by expressing the wave equation as

$$\hat{E}\psi = (\boldsymbol{\alpha} \cdot \hat{p} + \beta m)\psi \quad [1.3.3]$$

where the coefficient α has components corresponding to the momentum vector. Upon squaring both sides of (1.3.3), it can be shown that in order to satisfy the Einstein energy-momentum relationship, and therefore the Klein-Gordon equation, the coefficients in (1.3.3) must satisfy [9]

$$\begin{aligned}\alpha_x^2 &= \alpha_y^2 = \alpha_z^2 = \beta^2 = I \\ \alpha_j \beta + \beta \alpha_j &= 0 \\ \alpha_j \alpha_k + \alpha_k \alpha_j &= 0 \quad (j \neq k)\end{aligned}\tag{1.3.4}$$

In order for the relationships in (1.3.4) to be satisfied, the coefficients in (1.3.3) must be matrices. Furthermore, it is shown that these coefficients must be traceless, leading to the condition that the matrices describing these coefficients must be at least 4×4 antisymmetric matrices containing opposite spins and particle-antiparticle asymmetries. The coefficients are therefore defined in terms of the Pauli spin matrices σ_i as [3]

$$\beta \begin{pmatrix} I & 0 \\ 0 & -I \end{pmatrix} \quad \text{and} \quad \alpha_i = \begin{pmatrix} 0 & \sigma_i \\ \sigma_i & 0 \end{pmatrix}\tag{1.3.5}$$

where the Pauli spin matrices σ_i are represented as

$$\sigma_x = \begin{pmatrix} 0 & 1 \\ 1 & 0 \end{pmatrix}, \quad \sigma_y = \begin{pmatrix} 0 & -i \\ i & 0 \end{pmatrix}, \quad \sigma_z = \begin{pmatrix} 1 & 0 \\ 0 & -1 \end{pmatrix}$$

The 4×4 dimension of the operators now requires a four-component wave function, called the Dirac spinor [9]. It will be noted here that a relativistic treatment forces the wave function to have four components. Had equation (1.3.3) been evaluated with the assumption of a massless field, then 2×2 matrices would be acceptable solutions for the α coefficients as equation (1.3.5) gives the block representation of σ_i matrices, and the state fields could be properly described by a two component object. A covariant form of the Dirac equation can be written in a compact form as

$$(i\gamma^\mu \partial_\mu - m)\psi = 0 \quad [1.3.6]$$

where the gamma matrices γ^μ in (1.3.6) are defined by

$$\gamma^0 \equiv \beta, \quad \gamma^1 \equiv \beta\alpha_x, \quad \gamma^2 \equiv \beta\alpha_y, \quad \gamma^3 \equiv \beta\alpha_z$$

The four-component wave functions developed by Dirac provide a natural description of the intrinsic angular momentum of spin $\frac{1}{2}$ particles and antiparticles, and solutions for equation (1.3.6) for the free particle at rest yield positive and negative energy solutions, just as the Klein-Gordon equation did [9]. A detailed interpretation of the negative energy states is not in the scope of this thesis. However, it is worth noting that the four components are represented by spin-up and spin-down states for both particles and antiparticles. The four dimensional operators correspond to 4-momentum or 4-dimensional coordinate space, and the 4-component spinors correspond to 4-dimensional relativistic coordinates.

By taking relativistic effects into consideration, the wave functions of fermions are completely rewritten in the form of the Dirac spinors. In the following section, it will be determined that these relativistic effects will alter the energy levels that were determined by the Schrödinger equation.

Dirac Solution for Hydrogen Atom

The dynamics of electrons in a hydrogen atom is governed by the more formal approach of the Dirac equation. Solutions for the energy levels of electrons in a hydrogen atom are found by using equation (1.3.6) in a somewhat simplistic fashion, primarily with the intent that it will also verify the validity of the Klein-Gordon equation when dealing with energy states of the atom itself. Motivation for developing Dirac's equation was to give physical meaning to the probability densities described by the wave functions. This is what makes Dirac's equation more meaningful. However, in terms of

relativistic corrections to energies, both approaches will be valid to a certain extent. For the complete correction, only Dirac's approach can be used, as it incorporates spin corrections as well.

The Dirac equation with the incorporation of the hydrogen Coulomb potential is written as

$$\left[E + \frac{e^2}{r} - \boldsymbol{\alpha} \cdot \hat{\mathbf{p}} - \beta m \right] \psi = 0 \quad [1.4.1]$$

By multiplying both sides by $\left[E + \frac{e^2}{r} + \boldsymbol{\alpha} \cdot \hat{\mathbf{p}} + \beta m \right]$ and applying the commutation relations of the coefficients α and β , equation (1.4.1) can be written as [17]

$$\left[\left(E + \frac{e^2}{r} \right)^2 - \hat{\mathbf{p}}^2 - m^2 + i \boldsymbol{\alpha} \cdot \hat{\mathbf{r}} \frac{e^2}{r^2} \right] \psi = 0 \quad [1.4.2]$$

At this point spherical symmetry of the hydrogen atom is assumed, and it is useful to use a similar strategy as was done using the Schrödinger equation. For this purpose, the momentum operator is written in spherical coordinates, and the eigenvalues of the angular momentum operator are substituted in for the parts that are not dependent on position. Equation (1.4.2) can then be simplified to

$$\left[\left(E + \frac{e^2}{r} \right)^2 - \left(\frac{1}{r} \frac{d^2}{dr^2} r - \frac{l(l+1)}{r^2} \right) - m^2 + i \boldsymbol{\alpha} \cdot \hat{\mathbf{r}} \frac{e^2}{r^2} \right] \psi = 0 \quad [1.4.3]$$

Following a block diagonalization of the coefficient $\boldsymbol{\alpha}$ [17], it then follows that

$$\left[E^2 - m^2 + 2E \frac{e^2}{r} - \left(\frac{1}{r} \frac{d^2}{dr^2} r - \frac{l(l+1) + \alpha^2 \pm i \boldsymbol{\alpha} \boldsymbol{\sigma} \cdot \hat{\mathbf{r}}}{r^2} \right) \right] \psi = 0 \quad [1.4.4]$$

The numerator in the last term in the brackets includes the total spin of the electron j , which is a combination of the orbital and spin angular momentum. The third term in this

numerator commutes with \mathbf{J} , so it is useful to write the numerator in matrix representation as [17]

$$l(l+1) + \alpha^2 \pm i\alpha\boldsymbol{\sigma} \cdot \hat{\mathbf{r}} = \begin{pmatrix} \left(j + \frac{1}{2}\right)\left(j + \frac{3}{2}\right) + \alpha^2 & \mp i\alpha \\ \mp i\alpha & \left(j - \frac{1}{2}\right)\left(j + \frac{1}{2}\right) + \alpha^2 \end{pmatrix} \quad [1.4.5]$$

The eigenvalues of (1.4.5) are written as $\lambda(\lambda + 1)$ where the positive shift λ_+ and negative shift λ_- are determined to be

$$\lambda_+ = \left[\left(j + \frac{1}{2}\right)^2 - \alpha^2 \right]^{\frac{1}{2}} \quad \text{and} \quad \lambda_- = \left[\left(j + \frac{1}{2}\right)^2 - \alpha^2 \right]^{\frac{1}{2}} - 1 \quad [1.4.6]$$

In terms of just these eigenvalues and the radial terms, equation (1.4.4) becomes

$$\left[E^2 - m^2 + 2E \frac{e^2}{r} - \left(\frac{1}{r} \frac{d^2}{dr^2} r - \frac{\lambda(\lambda + 1)}{r^2} \right) \right] \psi = 0 \quad [1.4.7]$$

In comparing this equation to previous results, the energy levels of the Dirac equation are then given by

$$E_{nj} = m \left[1 + \left(\frac{\alpha}{n - (j + 1/2) + \sqrt{(j + 1/2)^2 - \alpha^2}} \right)^2 \right]^{-1/2} \quad [1.4.8]$$

It is easily shown that for $n = 1$, which can only correspond to $j = 1/2$, the principal energy level matches that given by equation (1.2.12). However, for higher energies, equation (1.4.8) shows that there is clearly breaking in the state degenerate in j that the Schrödinger solution would otherwise give. As a relevant example, the $n = 2$ level would allow for $j = 1/2$ and $j = 3/2$. Upon calculating the energy levels for these individual states, it is seen that there exists an energy difference of approximately 4.53×10^{-5} eV between the $2S_{1/2}$, or $2P_{1/2}$, and $2P_{3/2}$ states. This is a small, yet measureable, shift in the energy, and is known as the fine structure of hydrogen.

It is evident that under relativistic conditions, the spin effects of the fields must be taken into account in order to properly describe the structure of the hydrogen atom. The solution of the Dirac equation and the experimental measurement of the fine structure near 4.53×10^{-5} eV verify this notion. However, the Dirac equation still shows degeneracy for energies with similar j , but different l . Measurements made by Willis Lamb proved otherwise when he determined a shift between energies in the $2S_{1/2}$ and $2P_{1/2}$ states. The splitting of the $n=2$ lines to show fine structure and QED corrections is shown in Figure 1.2. Of course, this is known as the Lamb shift, and an in depth study of quantum field theory, specifically QED, is necessary before being able to properly determine the perturbative effects responsible for this shift. The next two chapters will focus primarily on these perturbative corrections. Following this, the structure is improved upon by taking temperature effects into consideration.

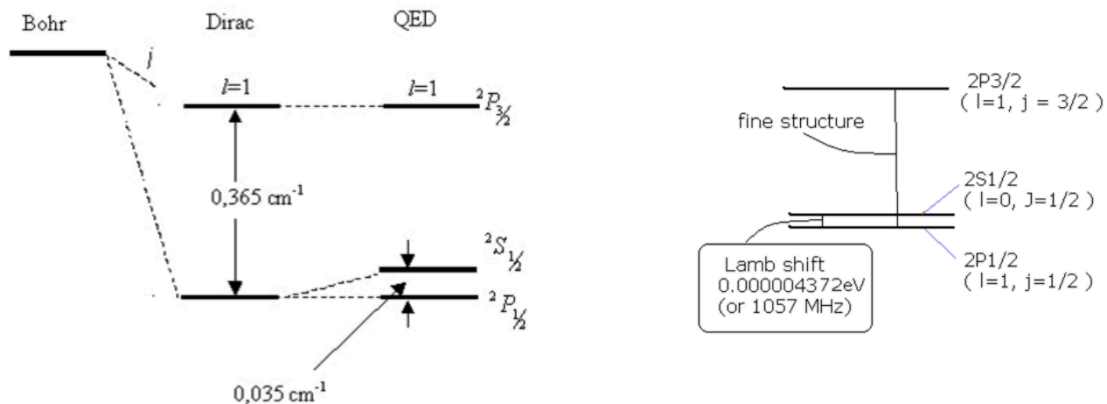


Figure 1.2 – Schrödinger, Dirac, and QED Energy Levels

(Left) The difference between results from Bohr (Schrödinger), Dirac and QED corrections for the $n=2$ state.

http://dydaktyka.fizyka.umk.pl/Wystawy_archiwum/z_omegi/lamba-en.html

CHAPTER II: QUANTUM FIELD THEORY

In the previous chapter, it was shown how the relativistic Klein-Gordon equation immediately provided a natural description for massless particles, something that was lacking in non-relativistic quantum mechanics. Dirac's relativistic formulation then provided a natural description for the spin of the electron, and experimental observation of the fine structure splitting helped to validate the necessity for a relativistic formulation of quantum mechanics. In this chapter a transition is made to field theory, and with this transition the propagator is used in preference to the wave function. The propagator, unlike the wave function, contains even more information since it describes how a particle travels from one location in space-time to another. This allows for the inclusion of the possible interactions that the particle may have during its journey from one location to another, and it will eventually be seen how these interactions lead to noticeable perturbative effects that otherwise cannot be accounted for by non-relativistic quantum mechanics. Though quantum field theory is a rather broad topic with many applications, the purpose of this chapter is to build a foundation that will ultimately allow for the theoretical calculation of the Lamb shift.

Perturbation Theory and the S-Matrix

The uncertainty principle in quantum mechanics allows for the violation of energy conservation so long as this violation happens in a sufficiently short period of time. In taking advantage of the uncertainty principle, it will prove to be useful and convenient to work in the interaction picture, rather than the Schrödinger picture. Note that the wave function in the interaction picture $\psi_I(t)$ is related to the wave function in the Schrödinger picture ψ_S by $|\psi(t)\rangle_I = e^{-\frac{i}{\hbar}H_0 t} |\psi(t)\rangle_S$. A transition to the field concept will be put off

for now. The Schrodinger equation can be written in the interaction picture in terms of just the potential as [1]

$$i\hbar \frac{d|\psi(t)\rangle_I}{dt} = \hat{V}_I(t)|\psi(t)\rangle_I \quad [2.1.1]$$

Being able to write the Schrödinger equation in terms of an interaction picture will allow for the focus to be placed on the perturbing potential and the effects it may have on the overall energy state. While solutions to the unperturbed state are already known, since the energy of an unperturbed particle in a state $|n\rangle$ must still obey the relation

$$\hat{H}_0|n\rangle = E_n|n\rangle \quad [2.1.2]$$

These values for the hydrogen atom were determined in chapter 1. The condition in (2.1.2) implies that the energy must be conserved beyond the limits of the uncertainty principle. The energy of the state of the particle before the perturbing interaction and the energy of the state of the particle following the interaction must be equal, and these should be equal to the energy of the unperturbed particle in (2.1.2).

Equation (2.1.1) can be written in terms of a time evolution operator by writing the interacting potential as $V_I = e^{\frac{i}{\hbar}H_0t}V_S e^{-\frac{i}{\hbar}H_0t}$, then the interacting wave function is written in terms of its initial state as

$$|\psi(t)\rangle_I = U_I(t, 0)|\psi(0)\rangle_I$$

where $U_I(t, 0)$ is referred to as the time translation operator. Of course, at this point it is necessary to begin to refer to the wave function as the field in order to reconcile the issues discussed in chapter 1 regarding the existence of the particle beyond its forward light cone. By substitution of equation (2.1.2) into equation (2.1.1) for the interacting field, the approximate solution for the time translation operator to nth order is [1]

$$\begin{aligned}
\hat{U}_I(t, t_i) = & \delta_{fi} - \frac{i}{\hbar} \int_{t_i}^{t_f} \hat{V}_I(t') dt' + \left(\frac{-i}{\hbar}\right)^2 \int_{t_i}^t \hat{V}_I(t_1) dt_1 \int_{t_i}^{t_1} \hat{V}_I(t_2) dt_2 + \dots \\
& + \left(\frac{-i}{\hbar}\right)^n \int_{t_i}^t \hat{V}_I(t_1) dt_1 \int_{t_i}^{t_1} \hat{V}_I(t_2) dt_2 \int_{t_i}^{t_2} \hat{V}_I(t_3) dt_3 \dots \int_{t_i}^{t_{n-1}} \hat{V}_I(t_n) dt_n + \dots
\end{aligned} \tag{2.1.3}$$

In making sense of the usefulness of the above equation, the transition probability from one state to the next is given by

$$P_{if}(t) = |\langle \psi_f | \hat{U}_I(t, t_i) | \psi_i \rangle|^2 \tag{2.1.4}$$

where the right-hand-side of equation (2.1.4) can be expanded in the form of (2.1.3). However, equation (2.1.4) is rarely expanded to include all of the terms seen in equation (2.1.3), and it is instead truncated to the second term in (2.1.3). The first term would of course yield zero in the requirement that the states will not be equal, and the higher order terms tend to vanish, as is the requirement if perturbation theory is to be valid.

Looking at the third term in equation (2.1.3), it is seen by the limits in the second integrand that t_2 is restricted to be less than t_1 . It would have been equally valid to write the interacting potential operator at t_1 to be within the second integrand, so long as it remains left of the interacting potential operator at t_2 . Then a theta function $\theta(t_1 - t_2)$ is introduced [1] to keep the order of time straight (this function is zero if $t_2 > t_1$) so that the upper limit of the second integrand is written simply as t . The second integrand in (2.1.3) now becomes

$$\int_{t_i}^t \hat{V}_I(t_1) dt_1 \int_{t_i}^{t_1} \hat{V}_I(t_2) dt_2 = \int_{t_i}^t dt_1 \int_{t_i}^t dt_2 \theta(t_1 - t_2) \hat{V}_I(t_1) \hat{V}_I(t_2) \tag{2.1.5}$$

Since the upper limits on the right-hand-side of equation (2.1.5) are no longer in terms of the differential elements, it is assumed t_1 and t_2 can be exchanged without loss of generality. This means that equation (2.1.5) could also be written like [1]

$$\int_{t_i}^t \hat{V}_I(t_1) dt_1 \int_{t_i}^{t_1} \hat{V}_I(t_2) dt_2 = \int_{t_i}^t dt_2 \int_{t_i}^{t_2} dt_1 \theta(t_2 - t_1) \hat{V}_I(t_2) \hat{V}_I(t_1) \quad [2.1.6]$$

Ultimately, this integral can be written as

$$\frac{1}{2!} \int_{t_i}^t dt_1 \int_{t_i}^{t_1} dt_2 [\theta(t_1 - t_2) \hat{V}_I(t_1) \hat{V}_I(t_2) + \theta(t_2 - t_1) \hat{V}_I(t_2) \hat{V}_I(t_1)] \quad [2.1.7]$$

Upon introducing the Wick time-ordering symbol T [1], which simply ensures that the operators are applied in the correct order, and recognizing that the coefficient with the factorial will increase by one with each additional term, the time translation operator is written in the much more compact and memorable form as

$$\hat{U}_I(t, t_0) = T e^{-\frac{i}{\hbar} \int_{t_0}^t dt' V_I(t')} \quad [2.1.8]$$

At this point it would be nice to develop an interacting Lagrangian and substitute it in to the above formula to ultimately determine the amplitudes generated by the interacting terms. Unfortunately, the purpose of separating the interacting part from the non-interacting free part is due to the unsolvable nature of the interacting part, as will be seen in later sections. Focus is now put on the interaction itself, which involves a scattering process during the translation of the field. The amplitude for a field beginning in a certain state and ending up in a final state will be defined by

$$a_{fi} = \langle f | \hat{S} | i \rangle \quad [2.1.9]$$

where \hat{S} is known as the S -matrix. The S -matrix is very similar to our time-evolution operator, but places emphasis on the interaction as a scattering process. As a reminder, the interacting part of the Hamiltonian is zero prior to and following the interaction. It is also assumed in scattering analysis that the particle is free long before and long after the scattering event. Thus, the conceptual basis behind treating the interaction as a scattering process is well-founded. Therefore, the S -matrix is the limit $\hat{S} = \hat{U}_I(t_2 \rightarrow \infty, t_1 \rightarrow -\infty)$, so that the S -matrix takes similar form as equation (2.1.8) as

$$\hat{S} = T e^{-i \int_{-\infty}^{\infty} d^4x \hat{\mathcal{H}}_I(x)} \quad [2.1.10]$$

where a slight alteration has been made to the integrand and interacting operator to make this more relativistically friendly. $\hat{\mathcal{H}}_I$ is the interacting Hamiltonian density, defined in chapter 1, and \hbar is taken to be equal to 1. Because the integral in equation (2.1.10) cannot be readily solved, it is often necessary to expand it back into a power series. The wonderful part about the S -matrix is that the operator within the matrix is the interacting operator, so the only terms in our Lagrangian or Hamiltonian that will be affected by the S -matrix are the parts separated from the free part.

In this section, a foundation has been set for determining perturbative effects from interactions that may exist while a field is translated through space. In the upcoming section, methods will be developed for how to handle these perturbations, and though many types of interactions may take place, emphasis will be placed on those interactions that are possible in QED processes.

The Propagator

Prior to understanding how the field will be perturbed, it is natural to first attempt to understand how the unperturbed field transitions from one point in space to another.

This amplitude is defined as the propagator. We will primarily be focusing on the amplitudes that a particle may begin at a given point y and end up at a point x , which can mathematically be written as $\langle x(t_x)|y(t_y)\rangle$. The relationship between the field and the amplitude at a position x is simply $\phi(x, t_x) = \langle x|\phi(t)\rangle$. Upon use of identity matrices, this is expanded in terms of the amplitude at another point in space and time as

$$\begin{aligned}\langle x|\phi(t)\rangle &= \langle x|e^{-iH_1t}|\phi\rangle = \int dy \langle x|e^{-i\hat{H}t}|y\rangle \langle y|\phi\rangle \\ &= \int dy \sum \langle x|\varphi_n\rangle e^{-i\hat{H}t} \langle \varphi_n|y\rangle \langle y|\phi\rangle\end{aligned}\quad [2.2.1]$$

The central sum in the integrand is a Green's function, and the final bracket is the amplitude for the particle at a position y at time t_y . To maintain physically reasonable results, the theta function may be inserted to ensure that time is forward, so more specifically the middle sum will be the time-retarded Green's function [1]. Equation (2.2.1) is now written as

$$\phi(x, t_x) = \int dy G^+(x, t_x, y, t_y) \phi(y, t_y) \quad [2.2.2]$$

where

$$G^+(x, t_x, y, t_y) = \theta(t_x - t_y) \sum_n \varphi_n(x) \varphi_n^*(y) e^{-iE_n(t_x - t_y)} \quad [2.2.3]$$

It is seen purely from how it is derived that this Green's function will contain more information than the wave function itself. It not only connects the initial and final states, but it also contains information on what happens between the initial and final states in the exponential function. From here on, this Green's function will be referred to as the propagator. The S -matrix in equation (2.1.10) will only operate on the field as it transitions from one state to the next. Therefore, the perturbations from the S -matrix will only operate on the propagator, since the states themselves correspond to the unperturbed

Hamiltonian density. Thus, a transition is made from the wave function/field mindset to that of the propagator.

The Green's function in equation (2.2.3) can be written in the frequency/energy domain as

$$G^+(x, y, E) = \lim_{\epsilon \rightarrow 0^+} \sum_n \frac{i\phi_n(x)\phi_n^*(y)}{E - E_n + i\epsilon} \quad [2.2.4]$$

where the pole is added to ensure causality [1].

The full propagator in equation (2.2.4) can be expanded in terms of a geometric series, and then reduced to the more memorable Dyson's equation as

$$G = G_0 + G_0VG_0 + G_0VG_0VG_0 + \dots = \frac{1}{G_0^{-1} - V} \quad [2.2.5]$$

where G_0 is the free propagator and V is the interacting potential. Similar steps could have been taken to derive the form of the propagator in momentum space, which would have resulted in

$$G_0^+(p, t_x, t_y) = \theta(t_x - t_y)e^{-iE_p(t_x - t_y)} \quad [2.2.6]$$

Upon taking a Fourier transform, the propagator as a function of energy and momentum is

$$G_0^+(p, E) = \frac{i}{E - E_p + i\epsilon} \quad [2.2.7]$$

The goal now is to develop the Feynman propagator, which will serve as a template for the fermion and photon propagators of QED. The Lagrangian density for a massless scalar field is given by [1]

$$\mathcal{L} = \frac{1}{2}(\partial_\mu)^2 \quad [2.2.8]$$

Upon insertion of equation (2.2.8) into the Euler-Lagrange equation (1.1.12), it is seen that solutions for the field components of this Lagrangian satisfy the wave equation

which propagate through space-time at the speed of light. A mass term can be included in (2.2.8) in the form of a potential energy as

$$\mathcal{L} = \frac{1}{2}(\partial_\mu)^2 - \frac{1}{2}m^2\phi^2 \quad [2.2.9]$$

Substituting equation (2.2.9) into equation (1.1.12) will give the Klein-Gordon equation, which was also derived in chapter 1 by introducing relativistic qualities to the Schrödinger equation. If an interacting source current J term is introduced to the Lagrangian density in equation (2.2.9), then the equations of motion have a similar structure to the Klein-Gordon equation in (1.3.2) as

$$(\partial_\mu\partial^\mu + m^2)\phi(x) = J(x) \quad [2.2.10]$$

In fact, an introduction of any interaction term to (2.2.9) will yield equations of motion that have very similar structure to equation (2.2.10), and in similar fashion, the interaction term can be separated out. Equation (2.2.10) is a non-homogenous differential equation. It is now relevant to define a Green's function Δ_F for equation (2.2.10) which satisfies

$$(\partial_\mu\partial^\mu + m^2)\Delta_F(x - y) = -\delta^{(4)}(x - y) \quad [2.2.11]$$

where the four-dimensional delta function on the right-hand-side of equation (2.2.11) can be expressed as

$$\delta^{(4)}(x - y) = \int \frac{d^4p}{(2\pi)^4} e^{-ip \cdot (x-y)}$$

This specific Green's function is defined to be the Feynman propagator. The solution for the Feynman propagator in (2.2.11) is then be shown to be equal to [1]

$$\Delta_F(x - y) = \lim_{\epsilon \rightarrow 0} \int \frac{d^4p}{(2\pi)^4} \frac{e^{-ip \cdot (x-y)}}{p^2 - m^2 + i\epsilon} \quad [2.2.12]$$

In separating the four-momentum variable in the denominator of (2.2.12), and using the expression for the relativistic energy in chapter 1, the propagator in equation (2.2.12) is written as

$$\Delta_F(x - y) = \int \frac{d^3\vec{p}}{(2\pi)^3} e^{-i\vec{p}\cdot(\vec{x}-\vec{y})} \int \frac{dp^0}{2\pi} \frac{e^{-ip^0\cdot(x^0-y^0)}}{(p^0 + E - i\epsilon)(p^0 - E + i\epsilon)} \quad [2.2.13]$$

The quantities in the denominator of expression (2.2.13) are meant to describe shifts from the real axis. The quantity on the left indicates a positive energy pole below the real-time axis, and the quantity on the right indicates a negative energy pole above the real-time axis. The locations of these poles will be of importance in the next chapter when performing a Wick rotation [1, 15]. The physical interpretation of the quantity on the left in (2.2.13) can be interpreted as positive energy moving forward in time (retarded Green's function) and the quantity on the right can be interpreted as negative energy moving backwards in time (advanced Green's function). Following Dirac's interpretation, the former positive energy state is considered to be a particle traveling from y to x where $x^0 > y^0$ and the latter negative energy state to be an antiparticle traveling from x to y where $y^0 > x^0$.

The Fourier component of equation (2.2.13) gives the Feynman propagator in momentum space to be [1]

$$\tilde{\Delta}_F(p) = \frac{i}{p^2 - m^2 + i\epsilon} \quad [2.2.14]$$

A key part of the physics behind all of this is that particles interact with one another by exchanging virtual particles. A virtual particle by definition is defined to be a particle that exists off mass-shell [1], which is only allowable by the uncertainty principle for $\Delta t \lesssim \hbar/E$. Virtual particles will then, of course, have a finite range for existence, which ends up being approximately equal to $1/m$ (or \hbar/mc in SI units) [1]. Since the focus of this paper is on QED, the virtual particles that control these interactions are

virtual photons, and the particles that the virtual photons interact with are, in the scope of this thesis, the electrons.

Quantum Electrodynamics

In quantum electrodynamics, focus is put solely on the interaction between the electromagnetic field and charged particles. The interactions between the virtual photons and the electron in QED are responsible for the Lamb shift, so the analysis of field theory will now be placed on this. The purpose of this section is to develop the propagators for the photon and electron, as well as a set of rules for how these propagators change through interacting scattering processes. This process begins with an in depth analysis of how a field transitions from one state to the next.

In general, the total amplitude for a particle to travel from one state to another is a sum over all possible trajectories, and can be described mathematically by the functional integral given by [1]

$$G = \int \mathcal{D}[q(t)] e^{i \int dt L[q(t)]} \quad [2.3.1]$$

where $\mathcal{D}[q(t)]$ is defined as

$$\mathcal{D}[q(t)] \equiv \lim_{N \rightarrow \infty} \prod_{n=1}^N \int \left(\frac{-im}{2\pi\Delta t} \right)^{1/2} dq_n \quad [2.3.2]$$

In classical mechanics, the stationary state dominates through variational principles, and is therefore given as the only possible path as predicted by Lagrange [16]. However, perturbative effects in quantum field theory cause the particle to shift slightly from this stationary state, resulting in quantum corrections. In order to determine the Green's functions for QED, it is necessary to determine a normalized generating

functional $\mathcal{Z}[J]$ which corresponds to the specific QED Lagrangian, where J is a source current.

In transitioning from particle trajectories $q(t)$ to field configurations $\phi(x)$, the action in (2.3.1) is now written in the form of the Lagrangian density from chapter 1. It is shown [1] that the normalized generating functional for the free scalar field is given by

$$\mathcal{Z}[J] = \frac{\int \mathcal{D}\phi e^{\frac{i}{2} \int d^4x \phi \{-(\partial^2 - m^2)\} \phi + i \int d^4x J \phi}}{\int \mathcal{D}\phi e^{\frac{i}{2} \int d^4x \phi \{-(\partial^2 - m^2)\} \phi}} \quad [2.3.3]$$

Though a term will need to be added later on for a full treatment of QED, the Lagrangian density for a massive field in electromagnetism is determined to be [1]

$$\mathcal{L} = -\frac{1}{4} F_{\mu\nu} F^{\mu\nu} + \frac{1}{2} m^2 A_\mu A^\mu \quad [2.3.4]$$

Where $F_{\mu\nu}$ is the electromagnetic field tensor $F_{\mu\nu} = \partial_\mu A_\nu - \partial_\nu A_\mu$, or

$$F_{\mu\nu} = \begin{pmatrix} 0 & E^1 & E^2 & E^3 \\ -E^1 & 0 & -B^3 & B^2 \\ -E^2 & B^3 & 0 & -B^1 \\ -E^3 & -B^2 & B^1 & 0 \end{pmatrix} \quad [2.3.5]$$

The massive electromagnetic field is used to determine the photon propagator. By substituting the Lagrangian density in equation (2.3.4) into the generating functional for the free scalar field in equation (2.3.3), it is determined that [1]

$$\mathcal{Z}[J] = \frac{\int \mathcal{D}A e^{\frac{i}{2} \int d^4x A^\mu \{(\partial^2 - m^2) g_{\mu\nu} - \partial_\mu \partial_\nu\} A^\nu + i \int d^4x J_\mu A^\mu}}{\int \mathcal{D}A e^{\frac{i}{2} \int d^4x A^\mu \{(\partial^2 - m^2) g_{\mu\nu} - \partial_\mu \partial_\nu\} A^\nu}} \quad [2.3.6]$$

The second term in the curly brackets is included to preserve gauge invariance. The homogenous form of the term in curly brackets would show that the generating functional is only related to the source current. Upon obtaining a Green's function solution to the

corresponding non-homogenous equation, and performing a Fourier transform, the propagator for the massive electromagnetic field in momentum space is [1]

$$\tilde{G}_{0\nu\lambda}(p) = \frac{-i(g_{\nu\lambda} - p_\nu p_\lambda/m^2)}{p^2 - m^2} \quad [2.3.7]$$

Before using equation (2.3.7) to determine the propagator for photons, it will be necessary to discuss gauge invariance in QED. In $U(1)$ symmetry, the conservation of fermion number must be conserved. Ultimately this leads to the conservation of current in QED. This notion of Gauge invariance, known as the Ward identity, will be an essential requirement for Feynman diagrams, which will be discussed in greater detail later on. For now, all that is needed to understand is that when the momentum vector k^μ is coupled to a fermion line, it cannot affect the current. Therefore, the dot product of k^μ with the S -matrix element corresponding to this interaction must be equal to zero.

Now, in the consideration of a virtual photon, which can be considered as a photon mediating the interaction between fermions, the second term in the numerator of equation (2.3.7) can be dropped by the Ward identity. Of course, this is a necessary step as we will now take the limit as $m \rightarrow 0$ of the propagator in (2.3.7), since the photon mass is assumed to be zero. Without use of the Ward identity, this would not give acceptable results for the photon propagator. Instead, the photon propagator is determined to be [2.3.8]

$$\tilde{D}_{0\mu\nu} = \frac{-ig_{\mu\nu}}{k^2 + i\epsilon}$$

The technique used to determine the photon propagator did not involve commutation relations with the operator, which is fine for photons since these are represented by Bose fields. However, a different approach must be made for fermions, since these fields in the canonical approach anticommute. The fermion will therefore be represented by Grassmann numbers, which anticommute. For the Grassmann-valued

vectors η , the generating functional in terms of the fields $\bar{\psi}$ and ψ , which will also appear as Grassmann numbers, is written as

$$Z[\eta, \bar{\eta}] = \int \mathcal{D}\psi \mathcal{D}\bar{\psi} e^{i \int d^4x [\bar{\psi}(x)(i\gamma^\mu \partial_\mu - m)\psi(x) + \bar{\eta}(x)\psi(x) + \bar{\psi}(x)\eta(x)]} \quad [2.3.9]$$

By completing the square for the term in the brackets of (2.3.9) [1], the normalized generating functional for the fermion can be written as

$$Z[\eta, \bar{\eta}] = e^{i \int d^4x d^4y \bar{\eta}(x)(i\gamma^\mu \partial_\mu - m)^{-1}\eta(y)} \quad [2.3.10]$$

Using the terms sandwiched between the Grassmann numbers in the integrand, the fermion propagator $S(x - y)$ is the solution to

$$(i\gamma^\mu \partial_\mu - m)iS(x) = i\delta^{(4)}(x) \quad [2.3.11]$$

The position space fermion propagator is then

$$G_0(x, y) = iS(x - y) = \int \frac{d^4p}{(2\pi)^4} \frac{ie^{-ip \cdot (x-y)}}{\gamma^\mu p_\mu - m + i\epsilon} \quad [2.3.12]$$

The momentum space fermion propagator is

$$\tilde{G}_0(p) = \frac{i}{\gamma^\mu p_\mu - m} = \frac{i(\gamma^\mu p_\mu + m)}{p^2 - m^2 + i\epsilon} \quad [2.3.13]$$

$$\tilde{G}_0(p) = \frac{i}{p^2 - m^2 + i\epsilon} \begin{pmatrix} m & p^0 - \mathbf{p} \cdot \boldsymbol{\sigma} \\ p^0 + \mathbf{p} \cdot \boldsymbol{\sigma} & m \end{pmatrix}$$

The second line in equation (2.3.13) is written to emphasize the fact that the propagator is four-dimensional, just as the Dirac spinors from chapter 1 were. Now that the free photon and fermion propagators have been determined, scattering processes in QED may now be discussed.

The scattering processes in QED between initial and final states are the causes of perturbations. Feynman diagrams are used to help simplify these scattering processes. The general QED interaction that this thesis focuses on is the coupling between the electromagnetic field and the electron, so determining the Feynman rules for the photon-fermion interaction is now a necessity. The Feynman Rules for fermions are shown in Figure 2.2 [1].

Before discussing the Feynman rules for QED, it is helpful to see how these rules are used to determine the amplitudes from the perturbations. A Dyson expansion of the S -matrix in equation (2.1.10) gives

$$\hat{S} = T \left[1 - i \int d^4z \hat{H}_I(z) + \frac{(-i)^2}{2!} \int d^4y d^4w \hat{H}_I(y) \hat{H}_I(w) + \dots \right] \quad [2.3.14]$$

Of course, the first term in this expansion corresponds to the unperturbed state. For scattering amplitudes, it is more useful to write the S -matrix instead as $\hat{S} = 1 + i\hat{T}$, where \hat{T} is the transition matrix (not to be confused with the time-ordering operator T). Since all future Feynman diagrams, as well as those in Figure 2.2, carry the energy and momentum conserving delta function, it is useful to define an invariant amplitude \mathcal{M} by

$$\langle p_{1f} p_{2f} | i\hat{T} | p_{2i} p_{1i} \rangle = (2\pi)^4 \delta^{(4)}(p_{1f} + p_{2f} - p_{1i} - p_{2i}) i\mathcal{M} \quad [2.3.15]$$

It will therefore only be necessary to calculate $i\mathcal{M}$ to determine the perturbative scattering effects.

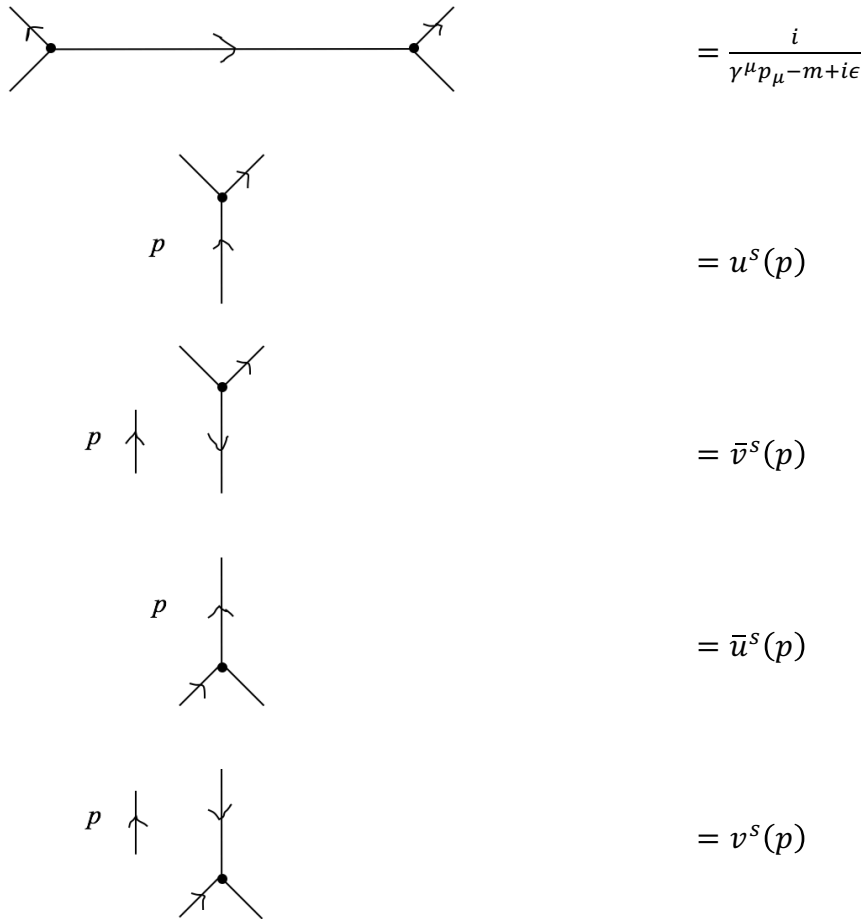


Figure 2.2 – Feynman Diagrams for Fermions: Each Feynman rule will contribute to the scattering amplitude, which will be discussed in more detail later on in this section.

At this point, the framework has been set for how the amplitudes will be calculated. Now the Feynman rules for the photon-fermion interaction will be discussed. This will provide sufficient background to determine the invariant amplitudes for QED processes that are responsible for the Lamb shift. The additional Feynman rules for QED are shown in Figure 2.3. It is important to note that in the scope of this thesis, the electron will always be considered to be bound, in which case the photons will always be

virtual, and the polarization tensor contributions $\epsilon_{\mu\lambda}$ and $\epsilon_{\nu\lambda}^*$ from the external photon lines will always be simplified to a metric tensor [1].

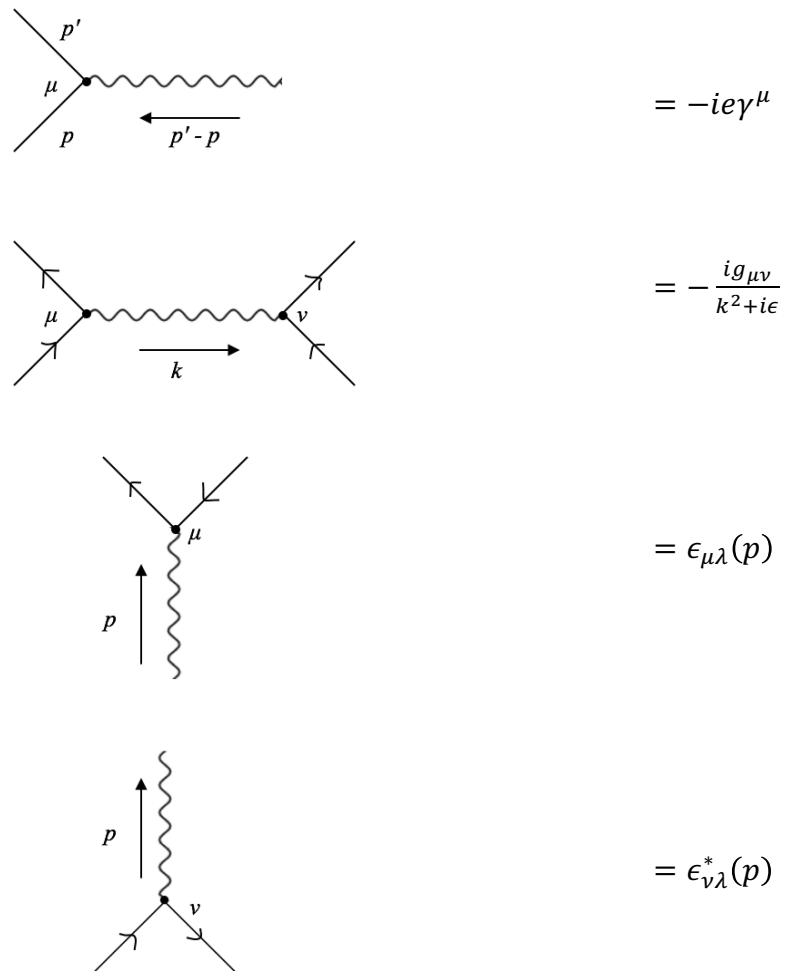


Figure 2.3 – Additional Feynman Rules for QED

These diagrams, along with those in Figure 2.4, give a complete list of rules to determine the corresponding invariant amplitude for an interaction in QED.

The simplest interaction in QED that will be involved in this paper is that between the electron and the proton in the hydrogen atom. Fortunately, the bound state energies for this system have already been solved. In a Feynman diagram representation, this

interaction would look similar to the second picture in Figure 2.3. In perturbation theory, at sufficiently high energies, Heisenberg's uncertainty principle may allow for processes such as the virtual photon splitting into electron-pairs. Theoretically, there may be no definite limit to how many times this can occur. It may also be possible under highly relativistic conditions for an electron to continuously emit and reabsorb photons that are not responsible for the coupling between the electron and proton in the hydrogen atom. By acknowledging these possibilities, it is found that the properties of the particles, such as mass and charge, are changed. In other words, an electron in a bound state does not have the same properties as a free electron.

It is obvious that if the intrinsic properties of the propagators are changed in an interaction, then the propagators themselves are changed. To determine the new propagators, one could simply determine the invariant amplitude from a scattering process by use of the Feynman rules, and calculate the new propagator. Unfortunately, this task is not so simple as it inevitably leads to divergent amplitudes, which implies that the electron and photon propagators are associated with an infinite amount of energy. It turns out that through a method called renormalization, these integrals are able to be solved. The next section is dedicated to discussing the process of renormalization, and conceptual reasons for why it is needed.

Before discussing renormalization, the Lagrangian describing fermions and their interactions should be developed in a more complete form. Since QED involves the interaction between fermions and the electromagnetic field, it seems reasonable to include this with the gauge field in the Lagrangian in (2.3.4). To include the interaction, a gauge field is introduced to the Dirac Lagrangian by the transformation

$$D_\mu = \partial_\mu + iqA_\mu(x) \quad [2.3.16]$$

The complete Dirac Lagrangian, which can be used to describe fermions and their interactions with the electromagnetic field, is then given by [1]

$$\mathcal{L} = -\frac{1}{4}F_{\mu\nu}F^{\mu\nu} + \bar{\psi}(i\gamma^\mu\partial_\mu - m)\psi - q\bar{\psi}\gamma^\mu A_\mu\psi \quad [2.3.17]$$

The second term in equation (2.3.17) is the Lagrangian that would give back the Dirac equation when substituted into the Euler-Lagrange equation. By including the first term, the third term must also be added to have local gauge invariance.

Renormalization

As was discussed previously, the interacting term in (2.3.17) will ultimately lead to divergent amplitudes in the electron charge. Reasons for infinite masses and charge are a consequence of transitioning to a field theory which allows particles to interact with the vacuum. The non-interacting particles are associated with what are defined as bare mass m_B , bare charge q_B , and bare fields ψ_B . These bare quantities are related to the physically measured quantities. For example, the physical mass m_P is related to the bare mass m_B by

$$m_P = m_B + \delta m \quad [2.4.1]$$

where δm represents the shift in mass due to the interactions. The bare quantities in quantum field theory must yield infinite results, because a completely unbound particle would correspond to an infinite amount of energy. Of course, this may not seem reasonable, but this is due to the fact that in field theory the particles will interact with the vacuum. Attempting to discuss the physical nature of a completely non-interacting field is unreasonable. For example, the charge of an electron will always have some screening effect associated with it due to virtual photons creating electron-positron pairs around the

electron. Quantum field theory innately contains divergences, and the solution to handling these divergences is renormalization.

Since the values of the properties of particles change through interactions, the properties must be renormalized. Of course, the renormalized quantities depend on the type of interaction. In the next chapter, the renormalized quantities are determined for QED, which can be accomplished by the addition of counterterms to equation (2.3.17). The counterterms themselves are also meant to represent infinite values, so that when added to the original Lagrangian density, only the physical terms survive. The actual process of carrying out the calculations in QED renormalization are done in the next chapter. In this section, prerequisite relationships between renormalization constants, bare quantities, and physical quantities are discussed.

The bare Dirac Lagrangian can be written as [15]

$$\mathcal{L} = -\bar{\psi}_B[\gamma^\mu \partial_\mu + m_B]\psi_B - V_B(\psi_B) \quad [2.4.2]$$

The renormalized field is defined through the renormalization constant Z_2 as

$$\psi \equiv Z_2^{-1/2}\psi_B \quad [2.4.3]$$

and the renormalized mass is defined by equation (2.4.1). The Lagrangian density is then rewritten in terms of these renormalized quantities as

$$\mathcal{L}_1 = -(Z_2 - 1)[\bar{\psi}[\gamma^\mu \partial_\mu + m]\psi] + Z_2 \delta m \bar{\psi}\psi - V_B(Z_2 \bar{\psi}\psi) \quad [2.4.4]$$

The specific values of these renormalization constants depend on the interaction process that the propagator goes through. The self-energy $\tilde{\Sigma}(p)$ of the fermion is defined as the interacting potential through a Dyson expansion of the propagator. The full propagator is simplified as a geometric series and can be written as

$$\tilde{G}_0(p) = \frac{i}{(i\gamma^\mu p_\mu)^2 - m^2 - \tilde{\Sigma}(p) + i\epsilon} \quad [2.4.5]$$

Since the position of the pole in the propagator defines the physical mass $m_p^2 = (\gamma^\mu p_\mu)^2$ for the non-interacting propagator, it is found that through the interaction the pole will be shifted by the inclusion of the self-energy term. Therefore, the physical mass will be shifted by

$$m_p^2 = m^2 + \tilde{\Sigma}(m^2 = (i\gamma^\mu p_\mu)^2) \quad [2.4.6]$$

It is implied by equation (2.4.6) that the physical mass and bare mass are identical when self-energy is zero. It may be useful to define the bare mass through the condition that the self-energy contribution is zero, such that

$$\tilde{\Sigma}(im) = 0$$

and

$$\left. \frac{\partial \tilde{\Sigma}(\gamma^\mu p_\mu)}{\partial (\gamma^\mu p_\mu)} \right|_{\gamma^\mu p_\mu = im} = 0 \quad [2.4.7]$$

The addition to the Lagrangian in (2.4.4) can be attributed to the self-energy contribution. In the next chapter, it will be shown how loop contributions are also included in this additional Lagrangian density. If there are no loop contributions, then the renormalization constants should be zero, to again give the physical mass and bare mass to be identical. The loop correction $\tilde{\Sigma}^*(im)$ is then attributed to the shift in mass by

$$Z_2 \delta m = -\tilde{\Sigma}^*(im) \quad [2.4.8]$$

and the renormalization constant Z_2 from the first term in (2.4.4) has the relation [15]

$$Z_2 = 1 - i \left. \frac{\partial \tilde{\Sigma}^*(\gamma^\mu p_\mu)}{\partial (\gamma^\mu p_\mu)} \right|_{\gamma^\mu p_\mu = im} \quad [2.4.9]$$

The self-energy of the photon $\tilde{\Pi}(q)$ can be determined in a similar fashion, and this is done in detail in the next chapter. The renormalization constant Z_3 associated with the renormalized electromagnetic field is defined by

$$A^\mu = Z_3^{-1/2} A_B^\mu \quad [2.4.10]$$

Since this renormalization constant is meant to characterize the effect on the charge, the renormalized charge is defined by

$$q = \sqrt{Z_3} q_B \quad [2.4.11]$$

The self-energy contributions to the fermion and photon propagator will ultimately have divergent amplitudes, which implies that the renormalized quantities will also give infinities. It is therefore necessary to subtract these terms from the Lagrangian, rather than simply using the new, renormalized values instead. In this sense, terms are not technically being added, but instead a shift is being made from the infinite quantities to the physical quantities. The free propagator realistically is not free, so what is assumed to be the bare mass is actually already taking some interactions into account. It is for this reason when analyzing a propagator in its bound state, one must be careful to not take these interactions into account again. This is what leads to the divergent amplitudes. Instead, these terms are subtracted from the interacting Lagrangian density through the process of renormalization.

Another correction that still needs to be made occurs at the photon-electron interaction vertex. Since relativistic field theory allows for the photon to split into electron-positron pairs, the vertex too needs to be corrected. This interaction is seen in the first picture of Figure 2.3. To allow for loop corrections, the vertex function will now be written as $-ie\tilde{\Gamma}^\mu(p, p')$, where the new vertex function is defined in terms of the form factors F_1 and F_2 as

$$\tilde{\Gamma}^\mu(p, p') = \gamma^\mu F_1(q^2) + \frac{i\sigma^{\mu\nu} q_\nu}{2m} F_2(q^2) \quad [2.4.12]$$

where $\sigma^{\mu\nu} = \frac{i}{2}[\gamma^\mu, \gamma^\nu]$ and $q^\mu = p'^\mu - p^\mu$ is the photon momentum. Hence, if the photon does not transfer momentum at the vertex, then $q = 0$, and in this case the Dirac form factor $F_1(0) = 1$ and the Pauli form factor $F_2(0) = 0$, which implies that the vertex function is equal to the first order contribution shown in Figure 2.3. It will be shown in the next chapter that there are higher order contributions to $F_2(0)$ which ultimately affect the electron magnetic moment and coupling constant.

CHAPTER III: RENORMALIZATION OF QED

Renormalization is a technique used to remove possible singularities in a theory that can appear through radiative corrections. Electron mass, wave function, and charge are renormalized, and the renormalization constants are calculated under different conditions. Renormalization of QED is followed by some radiative corrections leading to calculable perturbative effects.

In the previous chapter, we developed the Dirac equation, and the Dirac Lagrangian density that may describe the interaction between an electron and an electromagnetic field and is written in terms of the bare quantities as

$$\mathcal{L} = -\frac{1}{4}F_B^{\mu\nu}F_{B\mu\nu} - \bar{\psi}_B[\gamma_\mu(\partial^\mu + ie_B A_B^\mu) + m_B]\psi_B \quad [3.1]$$

The subscript B is added as a reminder that at the moment these quantities represent the fields, which have yet to be renormalized, of the interacting photon and electron, and the charge and mass of the electron. The relations of the renormalized fields, charge, and mass to their bare counterparts can be found in chapter 2. By the inclusion of counterterms, the Lagrangian is written as

$$\begin{aligned} \mathcal{L} = & -\frac{1}{4}F^{\mu\nu}F_{\mu\nu} - \bar{\psi}[\gamma_\mu\partial^\mu + m]\psi - ieA_\mu\bar{\psi}\gamma^\mu\psi - \frac{1}{4}(Z_3 - 1)F^{\mu\nu}F_{\mu\nu} \\ & - (Z_2 - 1)\bar{\psi}[\gamma_\mu\partial^\mu + m]\psi + Z_2\delta m\bar{\psi}\psi - ie(Z_2 - 1)A_\mu\bar{\psi}\gamma^\mu\psi \end{aligned} \quad [3.2]$$

The renormalization constants, fields, charge, and mass found in this Lagrangian will be determined in the upcoming sections.

Vacuum Polarization

One of the smaller, yet measurable, contributions to the Lamb shift comes from the renormalization of the photon propagator. Working with high-energy virtual photons results in the possibility that these photons can exist for sufficiently short periods as electron-positron pairs. If we look at the continuous Coulombic interaction between the electron and proton in the hydrogen atom, we can imagine that these high-energy, virtual photons exchanged between the electron and proton may form enough electron-positron pairs to contribute to electromagnetic properties. In essence, the vacuum should no longer be considered as “empty space” in relativistic field theory. The Feynman diagram describing this process is shown in Figure 3.1.

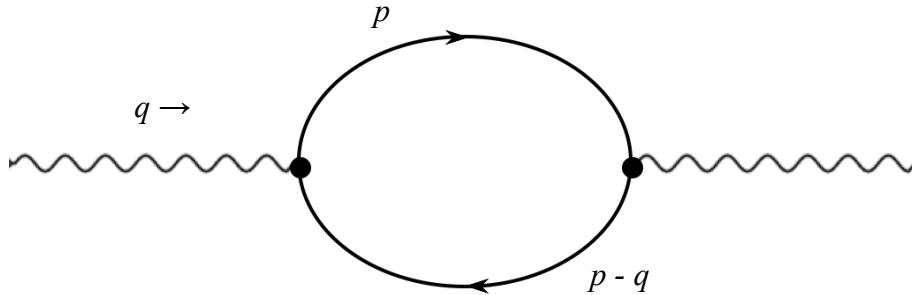


Figure 3.1 – Vacuum Polarization

1-Loop Feynman diagram describing vacuum polarization in QED. Wavy lines represent photons, and the solid lines represent incoming and outgoing electrons (positrons). [15]

The bare photon is now a dressed photon amidst the electron-positron pairs. To determine the propagator of the dressed photon, we begin with the Dyson expansion around the free photon propagator $\tilde{D}_{0\mu\nu}(q)$ so that the total photon propagator can be written as

$$\tilde{D}_{\mu\nu}(q) = \tilde{D}_{0\mu\nu}(q) + \tilde{D}_{0\mu\lambda}(q)[i\tilde{\Pi}^{\lambda\eta}(q)]\tilde{D}_{0\eta\nu}(q) + \dots \quad [3.1.1]$$

where $\tilde{\Pi}(q)$ is the 1PI photon self-energy. Upon insertion of the free photon propagator from the previous chapter, equation (3.1.1) becomes

$$\begin{aligned}\tilde{D}_{\mu\nu}(q) &= \frac{-ig^{\mu\nu}}{q^2} + \left(\frac{-ig_{\mu\lambda}}{q^2}\right) [i\tilde{\Pi}^{\lambda\eta}(q)] \left(\frac{-ig_{\eta\nu}}{q^2}\right) + \dots \\ &= \frac{-ig_{\mu\nu}}{q^2} + \left(\frac{-i}{q^2}\right) i\tilde{\Pi}_{\mu\nu}(q) \left(\frac{-i}{q^2}\right) + \left(\frac{-i}{q^2}\right) i\tilde{\Pi}_{\mu}^{\eta}(q) \left(\frac{-i}{q^2}\right) i\tilde{\Pi}_{\eta\nu}(q) \left(\frac{-i}{q^2}\right) + \dots\end{aligned}\tag{3.1.2}$$

The photon propagator is then given as $\tilde{D}_{\mu\nu}(q) = \frac{-ig_{\mu\nu}}{q^2} + \frac{1}{q^2} \tilde{\Pi}_{\mu\eta}(q) \tilde{D}_{\nu}^{\eta}(q)$ and the photon self-energy as $\tilde{\Pi}^{\mu\nu}(q) = (q^2 g^{\mu\nu} - q^{\mu} q^{\nu}) \tilde{\Pi}(q)$, which is acceptable since the Ward identity fixes the photon mass to zero. Ultimately, the renormalized photon propagator is written as

$$\tilde{D}_{\mu\nu}(q) = \frac{-ig_{\mu\nu}}{q^2 [1 - \tilde{\Pi}(q)]}\tag{3.1.3}$$

Since the photon self-energy term contains loops, it is necessary to involve counterterms while calculating $\tilde{\Pi}(q)$. It is determined that the calculation over a single electron-positron loop is sufficient and higher order calculations drop off rapidly [15]. The photon self-energy for a single loop is then defined to be $i\tilde{\pi}^{\mu\nu}(q) = i(g^{\mu\nu} q^2 - q^{\mu} q^{\nu}) \tilde{\pi}(q)$. The second-order QED counterterm for this is $i(g^{\mu\nu} q^2 - q^{\mu} q^{\nu}) C^{(2)}$ [1]. Since it is expected that the photon self-energy will vanish for $q^2 = 0$, it is implied that $\tilde{\pi}(q = 0) = -C^{(2)}$. The total photon propagator may then be written in terms of the 1-loop contribution as

$$\tilde{D}_{\mu\nu}(q) = \frac{-ig_{\mu\nu}}{q^2 [1 - [\tilde{\pi}(q) - \tilde{\pi}(0)]]}\tag{3.1.4}$$

The total photon propagator is meant to encompass the bare photon propagator and the interacting part which physically can be interpreted as the bare photon pulling electron-positron pairs from the vacuum. For a one-loop correction, this bare photon will

couple to a fermion line at each end of its trajectory, as seen in Figure 3.1. The previous statement is also true for multiple loop corrections, but in this schematic, higher order corrections are assumed to be negligible. To simplify the calculation, the Feynman vertex rules $-iQe_0\gamma^\mu$ are combined with the photon propagator. The photon propagator from (3.1.4) is then

$$\tilde{D}_{\mu\nu}(q) = \frac{-ig_{\mu\nu}e_0^2}{q^2[1 - [\tilde{\pi}(q) - \tilde{\pi}(0)]]} \approx \frac{-ig_{\mu\nu}e_0^2}{q^2}[1 + \tilde{\pi}(q) - \tilde{\pi}(0)] \quad [3.1.5]$$

where the approximation comes from a binomial expansion of the brackets in the denominator. In entertaining the idea that the photon may rip electron-positron pairs from the vacuum, it can be assumed that there is a type of screening involved in the vacuum, and this has perturbative effects on the Coulomb potential. This screening is referred to as vacuum polarization, and what follows is a detailed calculation to determine its contribution to the Lamb shift.

By incorporating the Feynman rules from chapter 2, the one-loop amplitude of the photon propagator is given as

$$i\tilde{\pi}(q) = (-1)(-ie_0)^2 \int \frac{d^4p}{(2\pi)^4} \text{Tr} \left(\gamma^\mu \frac{i}{p-m} \gamma^\nu \frac{i}{p+q-m} \right) \quad [3.1.6]$$

To begin the evaluation of (3.1.6), it is useful to write the equation in the form

$$i\tilde{\pi}(q) = (-1)(-ie_0)^2 \int \frac{d^4p}{(2\pi)^4} \frac{\text{Tr} \left((-i\gamma^\mu p_\mu + m) \gamma^\mu (-i(\gamma^\mu p_\mu - \gamma^\mu q_\mu) + m) \gamma^\nu \right)}{(p^2 + m^2 - i\epsilon)((p-q)^2 + m^2 - i\epsilon)} \quad [3.1.7]$$

Insight to the inclusion of the poles in the denominator was given in chapter 2. In an attempt to further simplify the integral in equation (3.1.7), the Feynman integral [15] is recognized as

$$\int_0^1 \frac{dx}{[(1-x)A + xB]^2} = \frac{1}{B-A} \left[\frac{1}{A} - \frac{1}{B} \right] = \frac{1}{AB} \quad [3.1.8]$$

Comparing equations (3.1.7) and (3.1.8), if $A = p^2 + m^2$ and $B = (p - q)^2 + m^2$, then equation (3.1.7) can be written in the slightly more solvable form as

$$\begin{aligned} i\tilde{\pi}(q) &= (-1)(-ie_0)^2 \int \frac{d^4p}{(2\pi)^4} \int_0^1 dx \frac{\text{Tr} \left((-i\gamma^\mu p_\mu + m)\gamma^\mu (-i(\gamma^\mu p_\mu - \gamma^\mu q_\mu) + m)\gamma^\nu \right)}{[(p^2 + m^2)(1-x) + ((p-q)^2 + m^2 - i\epsilon)x]^2} \\ &= (-1)(-ie_0)^2 \int \frac{d^4p}{(2\pi)^4} \int_0^1 dx \frac{\text{Tr} \left((-i\gamma^\mu p_\mu + m)\gamma^\mu (-i(\gamma^\mu p_\mu - \gamma^\mu q_\mu) + m)\gamma^\nu \right)}{[(p - qx)^2 + m^2 - i\epsilon + q^2x(1-x)]^2} \end{aligned} \quad [3.1.9]$$

The above equation may be simplified even further by making a change of variables through the transformation $p \rightarrow p + qx$,

$$= e_0^2 \int \frac{d^4p}{(2\pi)^4} \int_0^1 dx \frac{\text{Tr} \left((-i(\gamma^\mu p_\mu + \gamma^\mu q_\mu x) + m)\gamma^\mu (-i(\gamma^\mu p_\mu - \gamma^\mu q_\mu(1-x)) + m)\gamma^\nu \right)}{[p^2 + m^2 - i\epsilon + q^2x(1-x)]^2} \quad [3.1.10]$$

Gamma matrix identities, otherwise known as the Dirac identities, are used to simplify the numerator so that the metric tensor can be written in the form of inner products. A brief analysis of the denominator in the integrand would also entertain the idea of performing a Wick rotation [15]. Careful observation of equation (3.1.10) shows that if $m^2 + q^2x(1-x)$ is greater than zero over the interval from 0 to 1, then the poles of the propagator would be located at $p^0 = \pm\sqrt{p^2 + m^2 + q^2x(1-x) - i\epsilon}$, where the momentum under the root would depend only on the position coordinates. The Wick rotation must be performed counterclockwise so as to not cross the poles, so that the time component of the momentum is written as $p^0 = ip^4$, and the integration is performed over the entire imaginary axis, using the real limits for p^4 . Following the applications of the matrix identities and the Wick rotation [1, 15], equation (3.1.10) is written as

$$\begin{aligned}
i\tilde{\pi}(q) &= \frac{4e^2}{(2\pi)^4} \int_0^1 dx \int (d^4 p_E) [p^2 + m^2 + q^2 x(1-x)]^{-2} \\
&\times \left[-(p+qx)^\mu (p-q(1-x))^\nu + (p+qx) \cdot (p-q(1-x)) g^{\mu\nu} - \right. \\
&\quad \left. (p+qx)^\nu (p-q(1-x))^\mu + m^2 g^{\mu\nu} \right] \quad [3.1.11]
\end{aligned}$$

A rather convenient consequence of the Wick rotation is that the indices on the momentum vectors now run from 1 to 4, rather than 0 to 3, which allows for the integral to be evaluated using dimensional regularization, a technique developed by 't Hooft and Veltman [20]. Further techniques are used for simplification [15], ultimately allowing the integral to be written as a function of just p^2 , so that equation (3.13) becomes

$$\begin{aligned}
i\tilde{\pi}(q) &= \frac{4e^2 \Omega_d}{(2\pi)^4} \Gamma(d/2) \Gamma(2-d/2) (q^\mu q^\nu - q^2 g^{\mu\nu}) \\
&\times \int_0^1 dx x(1-x) (m^2 + q^2 x(1-x))^{\frac{d}{2}-2} \quad [3.1.12]
\end{aligned}$$

where Ω_d represents a sphere of d dimensions. Equation (3.1.12) still gives infinities for $d \rightarrow 4$, which makes this a convenient place to include the counterterm found in the fourth term on the right side of equation (3.2). The renormalization constant Z_3 can be determined using the original definition of the photon self-energy and the Ward identity. Ultimately, the photon self-energy can be written as [15]

$$\tilde{\Pi}(q) = \frac{e^2}{2\pi^2} \int_0^1 dx x(1-x) \ln \left(1 + \frac{q^2 x(1-x)}{m^2} \right) \quad [3.1.13]$$

It is worth mentioning at this point that the renormalization constant Z_3 is independent of the other two renormalization constants from equation (3.2) [15]. Therefore, the shift in energy due to vacuum polarization effects can be calculated prior to determining the self-energy of the electron and vertex corrections. There is a modification of the Coulomb potential with the renormalized propagator in (3.1.13). In evaluating the S -matrix corresponding to Figure 3.1, and comparing this with the Born

approximation for scattering, it is found that the potential in real space is related to the renormalized propagator by [15]

$$V(r) = \frac{e^2}{(2\pi)^3} \int d^3q e^{iq \cdot r} \left[\frac{1 + \tilde{\Pi}(q)}{q^2} \right] \quad [3.1.14]$$

It is seen that in the non-relativistic limit where the self-energy of the photon approaches zero, equation (3.1.14) reduces to the typical Coulomb potential. It can be shown that the renormalization of the photon propagator is, in essence, a renormalization of the Coulomb interaction, or the charge of the electron. Upon renormalizing the electric charge, it is found that the effective charge increases with decreasing length scale [1]. States with orbital quantum numbers $l = 0$ have non zero probability amplitudes near the origin of the orbit. Therefore, it is the S states that will be affected the most by vacuum polarization effects, and perturbative effects for $l > 0$ can be assumed to be negligible in comparison [15].

Via the interaction picture, the shift in energy due to vacuum polarization is written as

$$\Delta E = \int d^3r \Delta V(r) |\psi(r)|^2 \quad [3.1.15]$$

$$\Delta V(r) = \frac{e^2}{(2\pi)^3} \int d^3q e^{iq \cdot r} \left[\frac{\tilde{\Pi}(q)}{q^2} \right]$$

where $\Delta V(r)$ only involves the contribution from the relativistic correction. The shift in energy for the S states is found to be [15]

$$\Delta E_n = \frac{-4\alpha^5 m}{15\pi n^3} \quad [3.1.16]$$

The vacuum polarization contribution to the Lamb shift is then -1.12×10^{-7} eV, or -27.1 MHz. This effect alone does not come close to the experimental value, and it is

also contributing to an effective potential implying that an electron in the S state is more tightly bound to the atom. Vacuum polarization is definitely an important effect for charge renormalization, and it contributes to more accurate theoretical predictions of the Lamb shift. It will be seen in the following sections, however, that the self-energy of the electron and vertex corrections have much larger contributions.

As an extension of conceptual importance, a β -function may be introduced to observe how the coupling strength varies with distance. For an arbitrary choice of energy scale ξ , the β -function is then defined as [1]

$$\beta = \xi \frac{de}{d\xi} \quad [3.1.17]$$

The quantity in brackets in (3.1.5) is then assumed to be associated with the charge, solidifying the basis that it is the coupling constant which is corrected in the process of renormalizing the photon propagator. Therefore, the corrected charge is written as

$$e = e_0 [1 + \tilde{\Pi}(\xi)] \quad [3.1.18]$$

The logarithm term in equation (3.1.13) can be rewritten, and then the renormalized propagator is substituted into (3.1.18) to yield

$$e = e_0 \left[1 + \frac{-e^2}{2\pi^2} \int_0^1 dx x(1-x) \ln \left(1 + \frac{\xi^2 x(1-x)}{m^2} \right) \right] \quad [3.1.19]$$

The logarithm term was rewritten so that in the high energy limit ($\xi \gg m$), it becomes evident that upon differentiating with respect to the energy parameter

$$\frac{d\tilde{\Pi}(\xi)}{d\xi} = \frac{e_0^2}{\pi^2 \xi} \int_0^1 dx x(1-x) \quad [3.1.20]$$

Therefore, the β -function is determined to be

$$\beta = \frac{e_0^3}{12\pi^2} \quad [3.1.21]$$

The importance of the β -function is that it explicitly shows how the coupling strength will increase with increasing energy. Of course, this implies that with decreasing distance, the coupling strength increases. This is conceptually important to understanding why vacuum polarization gives a negative shift in the energy; it causes the electron to be more tightly bound. As it will be shown in the upcoming chapter, there may be external sources of energy which contribute to an increasing coupling strength. This is an important parameter which allows for bound states of hydrogen under extreme environmental conditions.

Electron Self-Energy

As the electron propagates through the vacuum it is constantly being bombarded by the virtual photons responsible for the coupling to the nucleus. This constant absorption and emission of photons will undoubtedly have an effect on the energy of the electron, and this will result in an effective mass different from the mass of an unbound electron. This is referred to as the physical mass, and calculation of this mass correction begins with the renormalization of the fermion propagator used to describe the electron. The fermion propagator was defined in chapter 2, and can be written in the form [15]

$$\tilde{S}(p) = [i\gamma^\mu p_\mu + m_e - \Sigma^*(p) - i\epsilon]^{-1} \quad [3.2.1]$$

where $\Sigma^*(p)$ is the 1-loop correction to the fermion propagator shown in Figure 3.2. It will be assumed for simplicity that higher order terms are negligible, so that the 1-loop

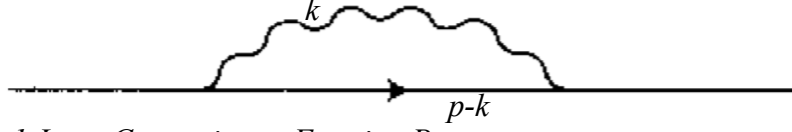


Figure 3.2 – 1-Loop Correction to Fermion Propagator

The 1-loop correction to the fermion propagator. The solid line here represents the electron, and the wavy line represents a photon being emitted and reabsorbed. [15]

correction gives the complete electron self-energy. Using the Feynman rules established in chapter 2, the 1-loop correction is written as

$$\Sigma^*(p) = \frac{ie^2}{(2\pi)^4} \int d^4k \left[\frac{1}{k^2 - i\epsilon} \right] \left[\frac{\gamma^\rho (-i\gamma^\mu p_\mu + i\gamma^\mu k_\mu + m_e) \gamma_\rho}{(p-k)^2 + m_e^2 - i\epsilon} \right] \quad [3.2.2]$$

Though dimensional regularization techniques can be used to solve this integral, it is found that a technique developed by Pauli and Villars [15] is more straightforward here. In this method, the photon propagator is separated into a low energy term and a high-energy as

$$\frac{1}{k^2 - i\epsilon} = \left[\frac{1}{k^2 + \mu^2 - i\epsilon} \right] + \left[\frac{1}{k^2 - i\epsilon} - \frac{1}{k^2 + \mu^2 - i\epsilon} \right] \quad [3.2.3]$$

The parameter μ in (3.2.3) is meant to represent a hypothetical photon mass.

Conceptually this parameter can be taken to infinity, in which case it would not affect the photon propagator. However, upon calculating the Lamb shift, it will be seen to be more convenient to make the claim that $m_e \gg \mu$ when evaluating low energy contributions.

The electron self-energy is then determined from the low energy contribution as

$$\Sigma^*(p) = \frac{ie^2}{(2\pi)^4} \int d^4k \left[\frac{1}{k^2 - i\epsilon} - \frac{1}{k^2 + \mu^2 - i\epsilon} \right] \left[\frac{\gamma^\rho (-i\gamma^\mu p_\mu + i\gamma^\mu k_\mu + m_e) \gamma_\rho}{(p-k)^2 + m_e^2 - i\epsilon} \right] \quad [3.2.4]$$

The denominators are combined in a form so that the Feynman integral in (3.1.8) may be implemented, and the gamma matrix identities are used, so that equation (3.2.4) is written in the more solvable form as [15]

$$\begin{aligned}
\Sigma^*(p) &= \frac{ie^2}{(2\pi)^4} \int d^4k [2i(\gamma^\mu p_\mu - \gamma^\mu k_\mu) + m_e] \\
&\times \int_0^1 dx \left[\frac{1}{((k - px)^2 + p^2(1-x) + m_e^2 x - i\epsilon)^2} \right] \\
&\times \frac{1}{((k - px)^2 + p^2 x(1-x) + m_e^2 x + \mu^2(1-x) - i\epsilon)^2}
\end{aligned} \tag{3.2.5}$$

The variable of integration is then shifted as $k \rightarrow k + px$ to get rid of the cross terms in the denominator, and a Wick rotation is performed so that (3.2.5) becomes [15]

$$\begin{aligned}
\Sigma^*(p) &= \frac{-2\pi^2 e^2}{(2\pi)^4} \int_0^1 dx [2i(1-x)\gamma^\mu p_\mu + 4m_e] \int_0^\infty d\kappa \kappa^3 \\
&\times \left[\frac{1}{(\kappa^2 + p^2 x(1-x) + m_e^2 x)^2} - \frac{1}{(\kappa^2 + p^2 x(1-x) + m_e^2 x + \mu^2(1-x))^2} \right]
\end{aligned} \tag{3.2.6}$$

Thus,

$$\begin{aligned}
\Sigma^*(p) &= \frac{-\pi^2 e^2}{(2\pi)^4} \int_0^1 dx [2i(1-x)\gamma^\mu p_\mu + 4m_e] \\
&\times \ln \left(\frac{p^2 x(1-x) + m_e^2 x + \mu^2(1-x)}{p^2 x(1-x) + m_e^2 x} \right)
\end{aligned} \tag{3.2.7}$$

In comparison with (3.1), and recognizing that the propagator in (3.2.1) should have a pole when $i\gamma^\mu p_\mu = -m_e$, the self-energy $\Sigma^*(p)$, mass correction δm_e , and renormalization constant Z_2 become [15]

$$\begin{aligned}
\Sigma^*(p) &= \frac{-\pi^2 e^2}{(2\pi)^4} \int_0^1 dx [2i(1-x)\gamma^\mu p_\mu + 4m_e] \ln \left(\frac{\mu^2(1-x)}{p^2 x(1-x) + m_e^2 x} \right) \\
\delta m_e &= \frac{2m_e \pi^2 e^2}{(2\pi)^4} \int_0^1 dx [1+x] \ln \left(\frac{\mu^2(1-x)}{m_e^2 x^2} \right)
\end{aligned} \tag{3.2.8}$$

$$Z_2 - 1 = \frac{2\pi^2 e^2}{(2\pi)^4} \int_0^1 dx \left\{ (1-x) \ln \left(\frac{\mu^2(1-x)}{m_e^2 x^2} \right) - \frac{2(1-x^2)}{x} \right\}$$

Therefore, the complete self-energy of the electron is determined to be absent of any ultra violet divergences as

$$\begin{aligned}
\Sigma(p) &= \Sigma^*(p) - (Z_2 - 1)(i\gamma^\mu p_\mu + m_e) + Z_2 \delta m_e \\
&= \frac{-2\pi^2 e^2}{(2\pi)^4} \int_0^1 dx [i(1-x)\gamma^\mu p_\mu + 2m_e] \ln \left(\frac{m_e^2(1-x)}{p^2 x(1-x) + m_e^2 x} \right) \\
&\quad - m_e [1+x] \ln \left(\frac{1-x}{x^2} \right) - (i\gamma^\mu p_\mu + m_e) \left[(1-x) \ln \left(\frac{1-x}{x^2} \right) - \frac{2(1-x^2)}{x} \right]
\end{aligned} \tag{3.2.9}$$

The mass correction in equation (3.2.8) can also be rewritten in the case where the photon mass is taken to be much less than the electron mass as [15]

$$\delta m_e \approx \frac{\alpha\mu}{2} \left[1 - \frac{3\mu}{2\pi m_e} \right] \tag{3.2.10}$$

Vertex Corrections and Anomalous Magnetic Moment

The next Feynman diagram to consider is shown in Figure 3.3. It is seen that the interaction between the electron and the virtual photon can be modified at the vertex. Again, this correction will be calculated to just first order, and higher orders will be assumed to be negligible. With this correction, the vertex factor will be transformed as

$$-ie\gamma_\mu \rightarrow -ie\gamma_\mu - ie\Gamma_\mu(p', p) \tag{3.3.1}$$

where $\Gamma_\mu(p', p)$ is the vertex function that can be written using Feynman rules as

$$\begin{aligned}
\Gamma_\mu(p', p) &= \int d^4k [e\gamma^\rho (2\pi)^4] \left[\frac{-i}{(2\pi)^4} \frac{-i(\gamma^\mu p_\mu - \gamma^\mu k_\mu) + m}{(p' - k)^2 + m^2 - i\epsilon} \right] \gamma^\mu \\
&\quad \times \left[\frac{-i}{(2\pi)^4} \frac{-i(\gamma^\mu p_\mu - \gamma^\mu k_\mu) + m}{(p - k)^2 + m^2 - i\epsilon} \right] [e\gamma_\rho (2\pi)^4] \left[\frac{-i}{(2\pi)^4} \frac{1}{k^2 - i\epsilon} \right]
\end{aligned} \tag{3.3.2}$$

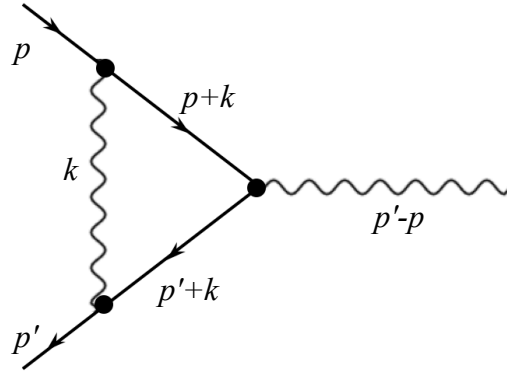


Figure 3.3 – Vertex Correction

An external virtual photon line interacts with the electron to result in a necessary correction to the vertex. The incoming solid line carries momentum p , while the external virtual photon line enters from above carrying momentum $q = p' - p$. The electron exits the interaction with total momentum p' .

The evaluation does involve dimensional regularization techniques, but rearranging the denominators will allow equation (3.3.2) to be written in a form similar to another Feynman integral given by

$$\frac{1}{ABC} = 2 \int_0^1 dx \int_0^x dy [Ay + B(x-y) + C(1-x)]^{-3} \quad [3.3.3]$$

Upon rewriting the denominator and shifting the variable of integration by $k \rightarrow k + p'y + p(x-y)$, the vertex function is determined to be [15]

$$\begin{aligned} \Gamma_\mu(p', p) = & \frac{2ie^2}{(2\pi)^4} \int_0^1 dx \int_0^x dy \int \frac{d^4k}{[k^2 + m^2x^2 + q^2y(x-y) - i\epsilon]^3} \\ & \times \gamma^\rho \left[-i \left(\gamma^\mu p'_\mu (1-y) - \gamma^\mu k_\mu - \gamma^\mu p'_\mu (x-y) + m \right) \right] \gamma^\mu \\ & \times \left[-i \left(\gamma^\mu p_\mu (1-x+y) - \gamma^\mu k_\mu - \gamma^\mu p'_\mu y \right) + m \right] \gamma_\rho \end{aligned} \quad [3.3.4]$$

Then a Wick rotation is performed in the counterclockwise direction, and the volume element d^4k is replaced with $2i\pi^2\kappa^3 d\kappa$ where κ is the Euclidean length of the four-vector k [15], giving the matrix elements between Dirac spinors to be

$$\begin{aligned}
\bar{u}'\Gamma_\mu(p', p)u &= \frac{-4\pi^2 e^2}{(2\pi)^2} \int_0^1 dx \int_0^x dy \int_0^\infty \kappa^3 d\kappa \\
&\times \bar{u}'\{\gamma^\mu[-\kappa^2 + 2m^2(x^2 - 4x + 2) + 2q^2(xy - y^2) + 1 - x] \\
&- 2im(p'^\mu + p^\mu)(x - x^2)\}u \\
&\times [\kappa^2 + m^2x^2 + q^2y(x - y)]^{-3}
\end{aligned} \tag{3.3.5}$$

Because this vertex correction stems from an external photon line, it will have contributions from the renormalized photon propagator from equation (3.1.13) by

$$\Gamma_{\mu, \text{vac}}(p', p) = \frac{1}{(p' - p)^2 - i\epsilon} \tilde{\Pi}(p' - p) \tag{3.3.6}$$

and the renormalization constant in (3.2) by

$$\Gamma_{\mu, \mathcal{L}}(p', p) = (Z_2 - 1)\gamma^\mu \tag{3.3.7}$$

It was also shown in chapter 2 that the vertex function in general can be written as a sum of the two form factor terms so that the matrix elements will also satisfy

$$\bar{u}'\Gamma_\mu(p', p)u = \bar{u}' \left[\gamma^\mu F(q^2) + \frac{i(p + p')^\mu}{2m} G(q^2) \right] u \tag{3.3.8}$$

From equations (3.3.5) through (3.3.6), the form factors are determined to be [15]

$$\begin{aligned}
F(q^2) &= Z_2 + \pi(q^2) + \frac{-4\pi^2 e^2}{(2\pi)^2} \int_0^1 dx \int_0^x dy \int_0^\infty \kappa^3 d\kappa \\
&\times \frac{\kappa^2 - 2m^2(x^2 - 4x + 2) - 2q^2(xy - y^2) + 1 - x}{[\kappa^2 + m^2x^2 + q^2(xy - y^2)]^3}
\end{aligned} \tag{3.3.9}$$

and

$$G(q^2) = \frac{-4\pi^2 e^2}{(2\pi)^4} \int_0^1 dx \int_0^x dy \int_0^\infty \frac{4m^2x(1-x)\kappa^3 d\kappa}{m^2x^2 + q^2(xy - y^2)} \tag{3.3.10}$$

For $q^2 = 0$, it must be true that $F(0) + G(0) = 1$. Another way of describing the process in Figure 3.3 is that a virtual photon decays into an electron-positron pair. Of course, by not including the 1-loop correction, this will result in $F(0) = 1$ and $G(0) = 0$. However, by including the possibility of the decay and following the perturbative QED procedures for the 1 loop correction to the vertex function, a vanishing q^2 does not results in $G(0) = 0$, and instead, upon evaluating (3.3.10), it is determined that

$$G(0) = \frac{-e^2}{8\pi^2} = \frac{-\alpha}{2\pi} \quad [3.3.11]$$

The magnetic moment operator is defined to be [1]

$$\hat{\mu} = [2F(0)] \frac{e^2}{2m} \hat{S} \quad [3.3.12]$$

where the quantity in brackets is known as the g -factor. Without perturbative QED corrections, $F(0)$ is simply 1, and $g = 2$. However, it is seen that corrections to the vertex predict the electron spin g -factor to be

$$g = 2[1 - G(0)] = 2 \left[1 + \frac{\alpha}{2\pi} \right] = 2.00232 \quad [3.3.13]$$

a result that has been experimentally verified, thereby once again proving the validity of QED treatment under relativistic conditions.

Substitution of the renormalization constant Z_2 from equation (3.2.8) into equation (3.3.9), and introducing the fictitious photon mass μ to the already existing terms in the integrand for $F(q^2)$, gives [15]

$$\begin{aligned}
F(q^2) = & 1 + \frac{e^2}{8\pi^2} + \pi(q^2) \\
& + \frac{2\pi^2 e^2}{(2\pi)^4} \int_0^1 dx \int_0^x dy \\
& \times \left\{ \frac{-m^2(x^2 - 4x + 2) - q^2[(xy - y^2) + 1 - x]}{m^2x^2 + q^2(xy - y^2) + \mu^2(1 - x)} + \frac{m^2[x^2 - 4x + 2]}{m^2x^2 + \mu^2(1 - x)} \right. \\
& \left. - \ln \left[\frac{m^2x^2 + q^2y(x - y) + \mu^2(1 - x)}{m^2x^2 + \mu^2(1 - x)} \right] \right\}
\end{aligned} \tag{3.3.14}$$

It will prove to be useful in the upcoming calculation of the Lamb shift to evaluate the expression in (3.3.9) in the infrared region for small q^2 . Then the first derivative of (3.3.9) at $q^2 = 0$ is [15]

$$\begin{aligned}
F'(0) = & \frac{e^2}{60\pi^2 m^2} + \frac{2\pi^2 e^2}{(2\pi)^4} \int_0^1 dx \int_0^x dy \\
& \times \left\{ \frac{-2y(x - y) + 1 - x}{m^2x^2 + \mu^2(1 - x)} + \frac{m^2[x^2 - 4x + 2]y(x - y)}{[m^2x^2 + \mu^2(1 - x)]^2} \right\}
\end{aligned} \tag{3.3.15}$$

where the first term is the vacuum polarization contribution, as it has a finite derivative at $q^2 = 0$. In evaluating the integral, it is determined that (3.3.9) yields

$$F'(0) = \frac{e^2}{24\pi^2 m^2} \left[\ln \left(\frac{\mu^2}{m^2} \right) + \frac{2}{5} + \frac{1}{4} \right] \tag{3.3.16}$$

and

$$G'(0) = \frac{e^2}{48\pi^2 m^2}$$

The Dirac form factor, defined in chapter 2, is then determined by the summation of equations (3.3.10) and (3.3.11) in the Taylor series expansion to be

$$F_1(q^2) \approx 1 + \frac{e^2}{24\pi^2} \left(\frac{q^2}{m^2} \right) \left[\ln \left(\frac{\mu^2}{m^2} \right) + \frac{2}{5} + \frac{3}{4} \right] \tag{3.3.17}$$

and the Pauli form factor to be

$$F_2(q^2) \approx \frac{e^2}{16m_e\pi^2} \quad [3.3.18]$$

These approximations for the form factors will prove to be very useful in the calculation of the Lamb shift, and it is important to note that the vacuum polarization contribution is taken into account in Dirac form factor. At this point, the tools necessary to calculate the Lamb shift have been developed. It has already been shown that energy shifts will be taking place, purely due to minor adjustments in the mass, charge, and magnetic moment of the electron. In the next section, it will be shown that the QED form factors can be separated into non-relativistic and relativistic corrections by evaluating the Dirac form factor contribution and Pauli form factor contribution respectively.

The Lamb Shift

The Dirac equation was solved in chapter 1 to show a breaking in the degeneracy between energy states corresponding to different total angular momenta. The sections of this chapter have shown higher orders in perturbation theory will have measureable contributions to these states. These radiative corrections lead to divergences in overall energy contributions to the electron, but special techniques involved in the renormalization of the propagators, such as dimensional regularization, help to cancel the ultraviolet divergences, i.e. the parameter μ is too large. However, this fictitious photon mass also gives infrared divergences if it is taken to be vanishing. The requirement for the photon mass in the Coulomb field is [15]

$$(Z\alpha)^2 m_e \ll \mu \ll Z\alpha m_e \quad [3.4.1]$$

In the high energy limit, the ultra-violet divergences are removed through the dimensional regularization techniques. Therefore, the form factors from the previous chapter can be used directly to determine the shift in energy in the high energy limit. Using the interaction picture, the shift in energy due to the correction in the Dirac form factor is given in position space by [15]

$$[\delta E_n]_{F_1} = \frac{-e^2}{24\pi^2 m_e^2} \left[\ln \left(\frac{\mu^2}{m_e^2} \right) + \frac{2}{5} + \frac{3}{4} \right] \int d^3 x f_n^\dagger(\mathbf{x}) [e \nabla^2 A^0(\mathbf{x})] f_n(\mathbf{x}) \quad [3.4.2]$$

Using $e \nabla^2 A^0(\mathbf{x}) = -Z e^2 \delta^3(\mathbf{x})$ and $[f_{njml}(0)]_\sigma = 2(Z \alpha m_e / n)^{3/2} \delta_{l,0} \delta_{\sigma,m} / \sqrt{4\pi}$, equation (3.4.2) is reduced to

$$[\delta E_{jnl}]_{F_1} = \frac{-2Z^4 \alpha^5 m_e}{3\pi n^3} \left[\ln \left(\frac{\mu^2}{m_e^2} \right) + \frac{2}{5} + \frac{3}{4} \right] \delta_{l,0} \quad [3.4.3]$$

In the presence of a pure electrostatic potential, the Pauli form factor contribution to the energy is determined in position space as [15]

$$[\delta E_n]_{F_2} = \frac{-ie^2}{32\pi^2 m_e} \int d^3 x (\bar{u}_n(\mathbf{x}) [\gamma, \gamma^0] u_n(\mathbf{x})) \cdot \nabla [e A^0(\mathbf{x})] \quad [3.4.4]$$

where the term in brackets is defined through the Pauli spin matrices by $\sigma^{\mu\nu} = \frac{i}{2} [\gamma^\mu, \gamma^\nu]$ [1]. Equation (3.4.2) and (3.4.4) are then combined to give the shift in energy in the high energy limit as

$$\begin{aligned} [\delta E_n]_{\text{high}} &= \frac{e^2}{24\pi^2 m_e^2} \left[\ln \left(\frac{\mu^2}{m_e^2} \right) + \frac{2}{5} \right] \int d^3 x f_n^\dagger(\mathbf{x}) [e \nabla^2 A^0(\mathbf{x})] f_n(\mathbf{x}) \\ &+ \frac{ie^2}{16\pi^2 m_e} \int d^3 x f_n^\dagger(\mathbf{x}) \boldsymbol{\sigma} \cdot (\nabla [e A^0(\mathbf{x})] \times \nabla f_n(\mathbf{x})) \end{aligned} \quad [3.4.5]$$

Now the low-energy contribution to the Lamb shift must be determined. In this process, the infrared divergence needs to be handled, as these divergences were not

cancelled out in the process of renormalization. The self-energy of the electron from section 2 in configuration space is given as [15]

$$\begin{aligned} \Sigma^*(p) = & \frac{ie^2}{(2\pi)^4} \int d^4k \gamma^\rho S_A(x, y; E - k^0) \gamma_\rho \times \left[\frac{1}{k^2 - i\epsilon} - \frac{1}{k^2 + \mu^2 - i\epsilon} \right] e^{ik \cdot (x-y)} \quad [3.4.6] \\ & - (Z_2(\mu) - 1)(\gamma \cdot \nabla + i\gamma^0 E + ie\gamma^\nu A_\nu + m_e) \delta^3(\mathbf{x} - \mathbf{y}) + \delta m_e(\mu) \delta^3(\mathbf{x} - \mathbf{y}) \end{aligned}$$

where $\delta m_e(\mu)$ and $Z_2(\mu)$ are defined by equation (3.2.8). Therefore, the low-energy contribution can be determined once again in the interaction picture as

$$\begin{aligned} [\delta E_n]_{\text{low}} = & \frac{-ie^2}{(2\pi)^4} \int d^4k \int d^3x \int d^3y \bar{u}_n(\mathbf{x}) \gamma^\rho S_A(x, y; E - k^0) \gamma_\rho u_n(\mathbf{y}) \quad [3.4.7] \\ & \times \left[\frac{1}{k^2 - i\epsilon} - \frac{1}{k^2 + \mu^2 - i\epsilon} \right] e^{ik \cdot (x-y)} + \delta m_e(\mu) \int d^3x \bar{u}_n(\mathbf{x}) u_n(\mathbf{x}) \end{aligned}$$

The electron propagator in equation (3.4.7) is written in the energy domain as the sum of the electron state and the positron state by

$$S_A(\mathbf{x}, \mathbf{y}; E) = \sum_m \frac{u_m(\mathbf{x}) \bar{u}_m(\mathbf{y})}{E_m - E - i\epsilon} - \sum_m \frac{u_m(\mathbf{x}) \bar{u}_m(\mathbf{y})}{E_m + E - i\epsilon} \quad [3.4.8]$$

By substituting equations (3.4.8) and (3.2.10) into (3.4.7) and evaluating the integral in (3.4.7) gives the low energy contribution as [15]

$$\begin{aligned} [\delta E_n]_{\text{low}} = & \frac{e^2}{2(2\pi)^3} \sum_m (E_m - E_n) |\mathbf{v}_{mn}|^2 \int d^3k \left[\frac{2}{3k^2(E_m - E_n + |\mathbf{k}| - i\epsilon)} \right. \quad [3.4.9] \\ & \left. - \frac{1 - \mathbf{k}^2/3(\mathbf{k}^2 + \mu^2)}{(\mathbf{k}^2 + \mu^2)(E_m - E_n + \sqrt{\mathbf{k}^2 + \mu^2} - i\epsilon)} \right] \end{aligned}$$

where \mathbf{v}_{mn} is the non-relativistic velocity operator. The integral in (3.4.9) is evaluated by invoking $(Z\alpha)^2 m_e \ll \mu$, where $(Z\alpha)^2 m_e \sim |E_m - E_n|$. This result gives an imaginary

part to the solution, which related to the non-zero probability that the atom will decay from state n to state m . Since only the real part of the solution is of interest in the calculation of the Lamb shift, the imaginary term is dropped, to give the low energy shift as

$$[\delta E_n]_{\text{low}} = \frac{e^2}{6\pi^2} \sum_m (E_m - E_n) |\mathbf{v}_{mn}|^2 \left[\ln \left(\frac{\mu}{2|E_n - E_m|} \right) + \frac{5}{6} \right] \quad [3.4.10]$$

The total energy shift is then the sum of equations (3.4.5) and (3.4.10), and is determined to be [15]

$$\begin{aligned} \delta E_n = & \frac{e^2}{6\pi^2} \sum_m (E_m - E_n) |\mathbf{v}_{mn}|^2 \left[\ln \left(\frac{\mu}{2|E_n - E_m|} \right) + \frac{5}{6} - \frac{1}{5} \right] \\ & - \frac{e^2}{16\pi^2 m_e^2} (\boldsymbol{\sigma} \cdot \nabla (eA^0(\mathbf{x})) \times \mathbf{p})_{nn} \end{aligned} \quad [3.4.11]$$

Now, specifically for the hydrogen Coulomb field, the amplitude for the transition between energy states n and m is

$$\sum_m (E_m - E_n) |\mathbf{v}_{mn}|^2 = \frac{e^2}{2m_e^2} (f_n^\dagger(0) f_n(0)) \quad [3.4.12]$$

which will only give contributions to electrons in the S states, $l = 0$. The matrix element for the magnetic term in (3.4.11) is

$$(\boldsymbol{\sigma} \cdot \nabla (eA^0(\mathbf{x})) \times \mathbf{p})_{nn} = -e \left(\frac{1}{r^3} \boldsymbol{\sigma} \cdot \mathbf{L} \right)_{nn} \quad [3.4.13]$$

which will only have non-vanishing contributions to the states other than S, or $l \neq 0$.

Since (3.4.11) will only contribute shifts based on quantum numbers in l , the analysis of the energy shift is separated for $l = 0$ and $l \neq 0$. It is straightforward to show that for the states with $l = 0$,

$$[\delta E]_{n,l=0} = \frac{4m_e\alpha^5}{3\pi n^3} \left[\ln \left(\frac{m_e}{2\Delta E_{n,l=0}} \right) + \frac{19}{30} \right] \quad [3.4.14]$$

where $\sum_m (E_m - E_n) |\mathbf{v}_{mn}|^2 \ln |E_n - E_m| \equiv \frac{e^2}{2m_e^2} \ln \Delta E_n (f_n^\dagger(0) f_n(0))$. For the states with $l \neq 0$, the shift in energy is determined to be [15]

$$[\delta E]_{jn,l \neq 0} = \frac{-4m_e\alpha^5}{3\pi n^3} \ln \left(\frac{2\Delta E_{jnl}}{m_e\alpha^2} \right) + \frac{m_e\alpha^5}{2\pi n^3} \left[\frac{j(j+1) - l(l+1) - \frac{3}{4}}{l(l+1)(2l+1)} \right] \quad [3.4.15]$$

where $\sum_m (E_m - E_n) |\mathbf{v}_{mn}|^2 \ln |E_n - E_m| \equiv \frac{2m_e\alpha^4}{n^3} \ln \left(\frac{2\Delta E_n}{m_e\alpha^2} \right)$. The mean excitation energies require numerical calculation, and for the 2S and 2P states, the mean excitation energies have been determined to be [15]

$$\Delta E_{2S} = 16.63934203 \frac{m_e\alpha^2}{2}$$

and

$$\Delta E_{2P} = 0.9704293186 \frac{m_e\alpha^2}{2}$$

[3.4.16]

Finally, the Lamb shift is determined to be

$$\Delta E(2S_{1/2} - 2P_{1/2}) = [\delta E]_{2S} - [\delta E]_{2P}$$

[3.4.17]

$$\Delta E(2S_{1/2} - 2P_{1/2}) = \frac{m_e\alpha^5}{6\pi} \left[\ln \left(\frac{\Delta E_{2P}}{\alpha^2 \Delta E_{2S}} \right) + \frac{91}{120} \right]$$

This gives the difference in energies to be approximately equal to 4.36×10^{-6} eV, or 1052 MHz, which is very close to the experimental result of 1057.8 MHz. Calculations involving higher-order radiative corrections, nuclear size, and recoil effects have given many numerically identical results to this amount of significant digits.

To this order in perturbation theory, the renormalized mass and first term in equation (3.4.7) cancelled. In this derivation, the cancellation of the renormalized mass term was necessary, as it was a function of the fictitious photon mass which was responsible for the unphysical divergences. It can also be argued that the mass correction must cancel, for if it did not, then an unreasonable energy shift would be calculated for an unbound electron. Calculations for the individual shifts in energy for each state would give

$$\delta E_{2S} = 4.30 \times 10^{-6} \text{ eV}$$

and

$$\delta E_{2P_{1/2}} = -5.34 \times 10^{-8} \text{ eV}$$

In the end, a large contribution to a positive shift in energy for the S-state wave function is responsible for the majority of the Lamb shift. Mathematically this is due to the fact that the delta function in (3.4.12) does not vanish for these states. Conceptually this can be attributed to the S-state wave functions overlapping with the nucleus, thereby giving greater relativistic contributions to the kinetic energy, which result in a slightly less bound electron. On the other hand, magnetic interactions for the P-state wave functions give electrons that are slightly more bound.

In the following chapter, it will be shown that thermal corrections to the mass and coupling constant can be written in forms that do not depend on these divergent terms, and contributions can therefore be added to equation (3.4.17) without working through the demanding process of cancelling divergences.

CHAPTER IV: LAMB SHIFT AT FINITE TEMPERATURE

The strong agreement between the experimental measurement and the theoretical calculation of the Lamb shift has arguably made quantum electrodynamics one of the most successful theories in modern physics. The perturbative interaction responsible for the Lamb shift is very small indeed, and as technology becomes more advanced and physicists continue to improve upon experimental techniques, greater concern needs to be taken from a theoretical standpoint in regards to what it means to be negligible. Formerly negligible external effects will not remain negligible so long as advancements in technology continue.

It has been shown that some problems of quantum mechanics cannot be resolved with the first quantization, and it is therefore necessary to look for the second quantization: the quantization of fields. Therefore, quantum field theory is unavoidable for the detailed understanding of QED systems, and the renormalization of QED has to be tested under given conditions. In reference to stellar cores and the early universe, QED renormalization is studied to assure the renormalizability of QED in the environmental conditions of such extreme astronomical systems.

In this chapter, existing calculations of temperature dependence on the Lamb shift which leads to unphysical contributions at temperatures of cosmological interest are reviewed. Results using the corresponding physically measurable effective parameters of QED are improved upon by calculating the finite temperature and density corrections of QED on the Lamb shift for the first time.

Blackbody Radiation Corrections to the Lamb Shift

The temperature dependency on the Lamb shift is a problem that has been previously approached. In this section, the attempts involving blackbody radiation and fluctuations in orbital position will be discussed in detail. A discussion follows as to why further improvements are required to properly describe the temperature dependency on the bound-state of the electron.

In an effort to determine the non-relativistic effects of blackbody radiation on the Lamb shift, the electron is allowed to interact with real photons from the surrounding medium, not just the virtual photons of the vacuum. This tiny effect of the Lamb shift is measurable in precision test experiments and theoretical and experimental results are in good agreement.

Knight [7] begins his calculation of thermal effects on the Lamb shift starting with the assumption that the interacting Hamiltonian can simply be written as the parts from a Hamiltonian describing charged particles in an electric field separated from the typical kinetic and potential energy terms, so that

$$\hat{H}_I = -\frac{e\hat{\mathbf{A}} \cdot \hat{\mathbf{p}}}{m} + \frac{e^2\hat{\mathbf{A}}^2}{2m} \quad [4.1.1]$$

where $\hat{\mathbf{A}}$ is the radiation field. In the previous chapter this interaction was expressed in terms of the electric dipole term. Though we have used similar interaction terms, the terms in (4.1.1) are meant to represent the interactions between the real photons and the electron.

The shift in energy due to the term on the right side of equation (4.1.1) can then be written as

$$\delta E_1 = \frac{e^2}{2m} \langle m | \hat{\mathbf{A}}^2 | m \rangle = \frac{\alpha}{\pi m} \int k dk \quad [4.1.2]$$

and the shift in energy to the first term on the right side of equation (4.1.1) can be written to accommodate the process of emission and absorption as

$$\begin{aligned}\delta E_2 &= \frac{e^2}{m^2} \sum_I \frac{\langle m | \hat{p} \cdot \hat{A} | n, k \rangle \langle n, k | \hat{p} \cdot \hat{A} | m \rangle}{E_m - (E_n - k)} \\ &= \frac{-2}{3\pi} \frac{\alpha}{m^2} \sum | \langle m | \hat{p} | m \rangle |^2 \int dk \left(1 - \frac{1}{1 + k/(E_n - E_m)} \right)\end{aligned}\quad [4.1.3]$$

where the second term of the integrand in equation (4.1.3) is meant to represent the radiative level shift. These shifts would be similar to what we would have obtained before, but now we include the effect of real photons of mode k . A transition to a statistical analysis is made by the inclusion of the photon occupation numbers, and equations (4.1.2) and (4.1.3) are now written as

$$\delta E_1 = \frac{2\alpha}{\pi m} \int k \bar{n}_k dk \quad [4.1.2a]$$

and

$$\delta E_2 = \frac{-4\alpha}{3\pi} \sum_n |v_{mm}|^2 \int_0^\infty dk k \bar{n}_k \left(\frac{\Delta E}{(\Delta E)^2 - k^2} \right) \quad [4.1.3a]$$

In the assumption that we will be dealing with a Bose-Einstein distribution of photons for black body radiation effects, \bar{n}_k (the mean number of photons in mode k , $\bar{n}_k = \frac{\sum_r n_r e^{-\beta E_r}}{Z}$) is defined through the canonical partition function, $Z = \mathcal{Z} = \prod_{k=1}^r (1 - e^{-\beta \epsilon_k})^{-1}$, and β is the typical thermodynamic quantity. The Bose-Einstein distribution then gives $\bar{n}_k = (e^{\beta \epsilon_k} - 1)^{-1}$. In combining equations (4.1.2a) and (4.1.3a), the total shift in energy in terms of the temperature T is written as

$$\delta E = \frac{-4\alpha}{3\pi} \sum_n \Delta E |r_{mn}|^2 T^2 \int \frac{x^3 dx}{(e^x - 1) \{ (\Delta E/T)^2 - x^2 \}} \quad [4.1.4]$$

In the low temperature limit, Knight shows that the shift in energy due to blackbody radiation is identically zero, while the shift in energy in the high temperature limit is

$$\delta E = \frac{-4\alpha}{3\pi} \sum_n \Delta E |r_{ms}|^2 T^2 \int \frac{x dx}{e^x - 1} = \frac{1}{3} \frac{\alpha \pi T^2}{m} \quad [4.1.5]$$

The shifts in energy could not be considered negligible in astronomical environments of extremely high temperature. However, since the shifts in energy have no dependence on energy level, each level will be shifted equally due to blackbody radiation effects. Therefore, according to equation (4.1.5), blackbody radiation will not produce observable corrections to the Lamb shift. Even though separation between the $2S_{1/2}$ and $2P_{1/2}$ levels may not increase, the result of (4.1.5) will still be valuable in determining the possibility of bound states for the electron.

As Knight points out, however, it has been determined that the external radiative field will still mix into the $2S_{1/2}$ and $2P_{1/2}$ states. Knight explores this idea and determines that in the high temperature limit such that the Lamb shift is much less than the temperature, $\Delta E \ll T$, there is a nonzero contribution to the Lamb shift itself. The shift in energy of the mixed states is given as

$$\delta E_{\text{mix}} = \frac{4\alpha}{3\pi} \Delta E (2S_{1/2} - 2P_{1/2}) |r_{mn}|^2 T^2 \frac{\pi^2}{6} \quad [4.1.6]$$

where $\Delta E (2S_{1/2} - 2P_{1/2})$ is the Lamb shift. The shift in energy in the high temperature limit is then given as the ratio $\frac{\delta E}{E} = \frac{4\pi T^2}{\alpha m^2}$.

Using the value for the Lamb shift obtained in the previous chapter, the correction to the Lamb shift due to blackbody radiation effects is

$$\Delta E^* (2S_{1/2} - 2P_{1/2}) = (4.379 \times 10^{-6} \text{ eV}) \left(1 + \frac{4\pi T^2}{\alpha m^2} \right) \quad [4.1.7]$$

where the uncorrected shift $\Delta E(2S_{1/2} - 2P_{1/2})$ is accepted as 4.379×10^{-6} eV . In the event that the temperature is much smaller than the electron mass, the contribution from blackbody radiation is negligible.

The mixing along with the shift given by (4.1.5) will not allow for bound states at these energies. Therefore, it is expected that hydrogen will be ionized and the Lamb shift will not be defined afterwards. Temperature corrections to the Lamb shift will have more contribution than the ionization energy and should no longer be considered as radiative corrections. However, under certain conditions the bound states may still exist, so the hypothetical correction due to blackbody radiation is plotted in Figure 4.1 below.

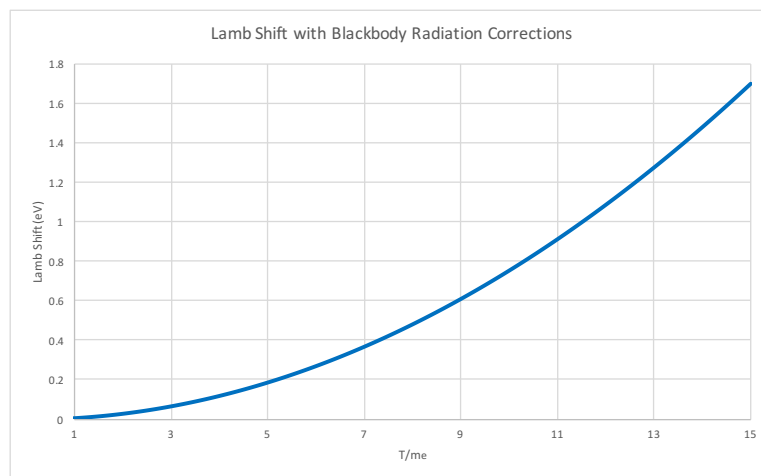


Figure 4.1 – Lamb Shift with Blackbody Radiation Corrections

The Lamb shift is plotted as a function of the ratio of T/m according to Knight's blackbody radiation corrections for the high temperature mixing between the $2S_{1/2}$ and $2P_{1/2}$ states.

If mixing takes place elsewhere, we may also have overlapping energy levels well before the ionization energy is reached. Knight also calculated the shift in the fine structure between the $2S_{1/2}$ and the $2P_{3/2}$ and showed the contribution here to be greater than it would be for the Lamb shift, so overlapping between the levels is not expected. It

is important to note here that the correction due to the mixing of the states is a perturbative effect independent of the Lamb shift, and the degeneracy between the $2S_{1/2}$ and $2P_{1/2}$ is broken at high temperatures before the consideration of relativistic effects responsible for the Lamb shift. Knight correctly argues these corrections to be negligible for common experimental practice. It is shown in Figure 4.1 that the difference between the $2S_{1/2}$ and $2P_{1/2}$ levels will continue to increase with increasing temperature without an apparent bound, though it is expected that the results from (4.1.5) will cause ionization before measureable shifts are possible.

Quantum Fluctuations and the Lamb Shift

Another possible perturbation is considered to be the fluctuation in the orbital position of the electron [11]. It may be considered that the fluctuations in the electromagnetic field will also create fluctuations in the kinetic and potential energies of the electron as it interacts with the field. These effects on the overall shifts in energy levels are determined in terms of the temperature [10, 11]. This will be a perturbative effect as well, because we consider the trajectory of the electron to be shifted due to the transformation $r \rightarrow r + \delta r$, where it should be assumed that $\langle \delta r \rangle = 0$. The instantaneous potential energy by this shift is given as $U(r + \delta r) = \left[1 + \delta r \cdot \nabla + \frac{1}{2}(\delta r \cdot \nabla)^2 + \dots \right] U(r)$. The average value of the potential energy $\langle U(r + \delta r) \rangle_{av} = \left[1 + \frac{1}{6} \langle (\delta r)^2 \rangle_{av} + \dots \right] U(r)$ can be written in terms of an exponential function as

$$\langle U(r + \delta r) \rangle_{av} = \exp\left(\frac{1}{6} \langle \delta r^2 \rangle \nabla^2\right) U(r) \quad [4.1.8]$$

In taking the potential energy as the typical Coulombic form $U(r) = -e^2/r$, then the shift in potential energy due to this perturbation is

$$\delta U_1(r) \approx \frac{2\pi}{3} e^2 \langle \delta r^2 \rangle \delta(r) \quad [4.1.9]$$

At this point we will now follow Kolomeisky's approach [10]. This approach is very similar to Welton's approach [11], but it also accounts for the shift in the potential energy if the electron exists within a distance that is less than the proton radius r_0 . It is useful that temperature effects are also included in this analysis. The potential energy for the electron within nucleus, assuming uniform charge density, is

$$U_2(r) = \frac{-e^2}{2r_0} \left(3 - \frac{r^2}{r_0^2} \right) \quad [4.1.10]$$

where r_0 is the radius of the proton and can be related to the Bohr radius a_B by $r_0 = (1.66 \times 10^{-5}) a_B$. Quantum mechanically, the electron is not allowed to exist inside of the nucleus, and it should be pointed out that the potential given by equation (4.1.10) is weaker than the Coulomb potential for the electron outside of the nucleus. Therefore, if the electron does exist at distances less than r_0 , an increase in the kinetic energy is expected, such that it will not remain within the nucleus for any appreciable amount of time. Because of the lack of r dependency, the first term in equation (4.1.10) will not contribute to any shift due to the Brownian motion of the electron, but the second term will contribute a shift given by

$$\delta U_2(r) = \frac{\alpha \langle \delta r^2 \rangle}{2r_0^3} \quad [4.1.11]$$

In the focus of the Lamb shift, the only states that will be effected by equations (4.1.9) and (4.1.11) are the S states, since the integration of the delta function with the P states will yield zero. Conceptually this should make sense, as the wave-function for the P states do not overlap with the proton. The physical implications of (4.1.11) put a lower bound on the motion. In the event that the scattering within the given orbital radius is

weak, perturbation theory seems to work very well. The strength of the barrier that determines whether the scattering is weak or not is written in the form of the dimensionless parameter λ as [10]

$$\lambda = \left((60241) \frac{\langle \delta r^2 \rangle}{a_B^2} \right)^{1/2} \quad [4.1.12]$$

This parameter will be related to scattering length caused by the proton-electron interaction. Kolomeisky then uses the Rydberg formula to determine the shift in energy due to what is defined to be the dimensionless quantum defect μ .

$$\Delta E_n(\mu) = \frac{1}{2(n - \mu_p)} - \frac{1}{2(n - \mu_s)} \quad [4.1.13]$$

$$\mu = -2(1.66 \times 10^{-5}) \left(1 - \frac{\tanh \lambda}{\lambda} \right) \quad [4.1.14]$$

It is now only necessary to calculate $\langle \delta r^2 \rangle$ to determine the resulting contributions to the Lamb shift. Kolomeisky does this by assuming a non-relativistic harmonically bound electron, and then improves upon Welton's equation of motion for the electron by including a radiation damping term. By incorporating the fluctuation-dissipation theorem, and the mean-square fluctuation can be written in integral form as

$$\langle \delta r^2 \rangle = \frac{3\hbar}{\pi} \int_0^\infty d\omega \mathcal{A}''(\omega) \coth\left(\frac{\hbar\omega}{2T}\right) \quad [4.1.15]$$

where ω is the oscillation frequency meant to represent the motion about the Bohr orbit, and T is the temperature, and $\mathcal{A}''(\omega)$ is the generalized susceptibility [13]. By using the same cutoff frequency as Welton [11], the mean-square displacement of the electron as a ratio to the Bohr orbit is determined to be [10]

$$\frac{\langle \delta r^2 \rangle}{a_B^2} = \frac{2\alpha^3}{\pi} \ln \frac{n^3}{\alpha^2} \quad [4.1.16]$$

Upon calculating this ratio for the $n=2$ state, it is determined that the mean-square displacement is approximately 0.0017 times the size of the Bohr radius, thus implying perturbation theory to be valid. Equation (4.1.16) is substituted into equation (4.1.12) to determine the dimensionless barrier strength. For the $2S_{1/2}$ state the barrier strength is calculated to be approximately 0.4216. The quantum defect for this state is then determined to be approximately $\mu_S = 1.86 \times 10^{-6}$, and the $2P_{1/2}$ state is assumed to be unaffected by the barrier for reasons discussed earlier, thereby giving a defect $\mu_P = 0$. The corresponding shift in energy due to the fluctuation in the position of the electron in the $2S_{1/2}$ state is then determined to be approximately -2.30×10^{-7} eV, or -55.6 MHz. This predicted shift due to fluctuations is near 5% of the overall value of the Lamb shift, and like vacuum polarization, is in the opposite direction.

With the approximation that $\coth(x) \approx 1/x$ for $x < 1$ and $\coth(x) \approx 1$ for $x \geq 1$, the evaluation equation (4.1.15) would instead give the shift in terms of the temperature as

$$\langle \delta r^2 \rangle \approx 3T^2 n^6 + \frac{2\alpha^3}{\pi} \ln \left(\frac{1}{T\alpha^2} \right) \quad [4.1.17]$$

The second term on the right-hand-side is meant to represent contributions from quantum fluctuations, while the first term is the classical contribution. The temperature in (4.1.17) is measured in a.u., so $T = 1$ a.u. corresponds to 3.158×10^5 K. The contribution to the Lamb shift due to quantum fluctuations can be seen in Figure 4.2, noting that these contributions will result in negative energy shifts, similar to vacuum polarization. Thermal corrections due to quantum fluctuations in electron orbit become negligible as temperatures approach 0.511 MeV. This can be attributed to the increase in orbital radius as the overall energy state increases, thereby reducing a noticeable change in potential.

At these temperatures, the perturbation used becomes negligible, and higher order terms from equation (4.1.8) would need to be considered.

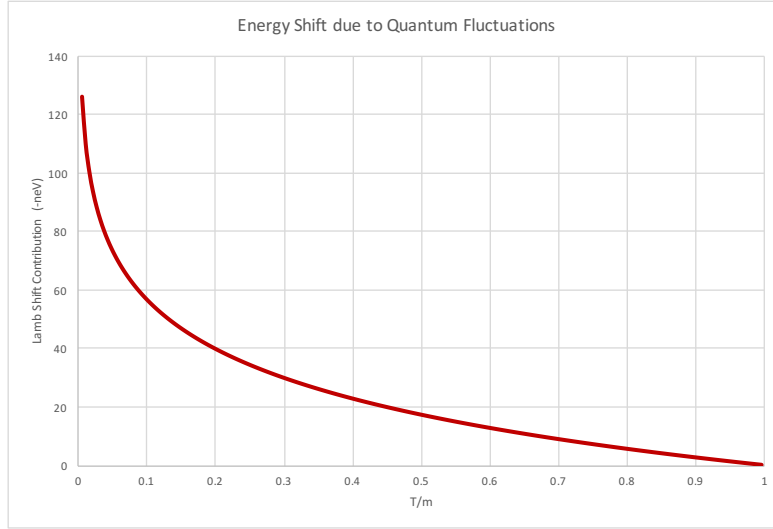


Figure 4.2 – Lamb Shift due to Quantum Fluctuations

A possible contribution to the Lamb shift due to quantum fluctuations.

It must be noted that equation (4.1.17) cannot be valid for any value of n , as the state would eventually become unstable with increasing shifts in the displacement. We must require that $\langle \delta r^2 \rangle$ remain sufficiently small, so that the electron does not fluctuate to the point where it is no longer bound. One constraint that must be applied is $Tn^2 \ll 1$ to accommodate the previous condition. Another constraint that must be applied is $n \ll \alpha^{-3}T^{-1}$ to ensure that the state does not decay before it can be measured. The range for principal quantum numbers is therefore $T^{-1/3} \ll n \ll T^{-1/2}$ [10]. One interesting application of this would be to show that at room temperature, this effect is valid for quantum numbers n between 10 and 31. States for $n < 10$ would still be considered stable, but the integration technique to develop equation (4.1.17) would no longer be valid, as it assumed sufficiently high temperatures. A contribution from the fluctuations

to the Lamb shift at room temperature would then be unobservable. With greater attention to the Lamb shift, the upper temperature limit for the $n=2$ level would be 78,950 K, or 6.81 eV, which is well below our consideration for high temperatures. It may also be worth noting that if these temperatures were taken into consideration, the shifts in energy would be dominated by the classical term in equation (4.1.17). Regardless of the validity of (4.1.17) at these temperatures, the contributions to the Lamb shift would be well beyond the ionization energy due to the classical contribution.

By working in ranges of non-relativistic quantum, Knight determines that each state will be equally shifted in the high temperature limit, and contributions to the Lamb shift will be null. In the following chapter, the temperature dependency on the electron mass and coupling constant will suggest otherwise. However, a result that will still prove to be useful in the section that follows is the temperature dependent shift due to the mixing of the states, which occurs prior consideration of the Lamb shift. Careful consideration will also be given to Kolomeisky's approach involving the mean-square fluctuation of the electron. Though caution must be taken in considering the validity of the classical approaches taken, the contributions to the Lamb shift on similar scales to vacuum polarization are too interesting to ignore, and will be briefly discussed in the following section. However, it has been determined that at sufficiently high temperatures, fluctuations in the orbital motion of the electron do become negligible, and will therefore not be taken into account for final conclusions.

Renormalization of QED at Finite Temperature and Density

Renormalization of QED in hot and dense medium is studied using the real-time formalism where an order-by-order cancellation of singularities can be explicitly shown, and the Kinoshita-Lee-Nauenberg (KLN) theorem can be proved explicitly as order-by-

order calculations of all diagrams. Explicit calculations of the renormalization constant of QED in different conditions of temperature and chemical potential are presented in literature in detail [14, 29]. The renormalization constants of QED including electron mass, electron charge and electron wave function are evaluated as a function of temperature and chemical potential. These can be used as physically measurable and effective parameters of the theory.

It was shown in chapter 3 that the relativistic electron interacts with the electromagnetic field in such a way so as to shift the energy of the atom. It should then be useful to explore the possibilities that other factors, such as temperature, may also contribute to shifts in this energy. In a many particle relativistic system at extremely high temperature and chemical potential, renormalization scheme helps to evaluate QED parameters at $T \ll m_e$ and $T \gg m_e$ ($\sim 10^{10}$ K). The chemical potential μ is also expressed in terms of electron mass (chemical energy of 0.511 MeV). QED parameters have been calculated for the relevant ranges of T and μ .

Calculations of renormalized constants in the many body relativistic system include only electrodynamic interactions. The QED fluid changes the physical values of parameters including the coupling constant α . This leads to the change in the electromagnetic properties of the system including electric permittivity, magnetic permeability and magnetic moment of charged particles. Due to these changes in the QED medium at extremely high temperature and density, radiative corrections stemming from external interactions may contribute to measurable energy shifts in the hydrogen atom. The bound states of hydrogen are possible to exist at higher temperatures only if chemical potential is also extremely high and is larger than the temperature. Such systems are available in neutron stars and supernovae, so calculation of the Lamb shift is relevant to study in highly dense stellar cores.

Calculation of temperature dependence on the Lamb shift is therefore an interesting topic. However, experimental measurement of the Lamb shift has always been challenging due to it being such a small factor. Regardless of the difficulties in measurements, these calculations may be very helpful to understand the interior structure of compact objects and we can interpret the observational results in a much more accurate way. Thermal corrections and density dependence is expected to help in precision, but a persistent perturbative effect may give sizeable corrections which cannot be ignored.

The renormalization of the particles propagating through the vacuum have already been calculated, and will furthermore be considered as solutions prior to the interaction in the hot, dense media. In the systems of interest, the particles cannot be considered freely propagating, bare particles. When statistical background energies are around the threshold energies sufficient for electron-positron pair production, a continuous exchange of electrons and photons between particles generate thermal effects that must be taken into account. Statistical effects are introduced through Dirac-Fermi and Bose-Einstein distributions. The photon and fermion propagators from chapter 3 are statistically corrected through these distributions respectively by [18]

$$D_{\beta}(q) = \frac{i}{q^2 - m^2 + i\epsilon} + \frac{2\pi}{e^{\beta E_q} - 1} \delta(q^2 - m^2) \quad [4.2.1]$$

$$S_F(p) = \frac{i}{(\gamma^{\mu} p_{\mu})^2 - m^2 + i\epsilon} + \frac{2\pi(\gamma^{\mu} p_{\mu} + m)}{e^{\beta E_p} - 1} \delta(p^2 - m^2) \quad [4.2.2]$$

As was discussed previously, the vacuum corrections to the first terms in equations (4.2.1) and (4.2.2) have already been calculated, so thermal contribution to the renormalized mass can be separated as

$$m_R = m + \delta m(T = 0) + \delta m(T) \quad [4.2.3]$$

Through the processes discussed above, Masood determines [14] that in the low temperature limit for $T \ll m$ and the high temperature limit $T \gg m$, the thermal contributions in (4.2.3) can be written in the forms

$$\frac{\delta m(T)}{m} \approx \frac{\alpha \pi T^2}{3m^2} \quad T \ll m \quad \text{and} \quad \frac{\delta m(T)}{m} \approx \frac{\alpha \pi T^2}{2m^2} \quad T \gg m \quad [4.2.4]$$

As it might be expected, the rate of change of the mass as a function of temperature is larger for temperatures greater than the electron mass. At these temperatures, contributions from external radiative effects tend to dominate the fermion background contributions.

The charge renormalization does not alter the coupling constant for $T \ll m$, and for $T \gg m$ it is given by [14]

$$\alpha(T) = \alpha(T = 0) \left(1 + \frac{\alpha^2 T^2}{6m^2} \right) \quad T \gg m \quad [4.2.5]$$

This increasing coupling constant will correspond to an increasing effective charge, thereby allowing for bound states beyond the typical expected background energies.

In the event that the environments of interest are also extremely dense, then the growth of the mass is expected to be inhibited as the high densities will result in smaller mean paths. A large enough chemical potential will also overcome thermal effects altogether. This is seen in the corrected Fermion distribution function with the inclusion of the chemical potential as

$$n_F(p + \mu) = \frac{1}{e^{-\beta(E_p + \mu)} + 1} \quad [4.2.6]$$

Therefore, in the event that the chemical potential is sufficiently high, it may follow that $\mu \gg T > m$, implying that the thermal mass correction has been suppressed by the

overbearing chemical potential. The self-mass correction under this condition has been calculated by Masood [19] in terms of the chemical potential, and is given as

$$\frac{\delta m}{m}(T, \mu) \simeq \frac{3\alpha}{\pi} \ln \frac{\mu}{m} + \frac{\alpha}{\pi} \left(1 - \frac{\mu^2}{m^2}\right) \left(3 \frac{m^2}{\mu^2} + \frac{2p^2}{\mu^2} - 1\right) \quad [4.2.7]$$

so that for extremely large values of chemical potential,

$$\frac{\delta m}{m}(T, \mu) \simeq -\frac{\alpha \mu^2}{\pi m^2} \quad [4.2.8]$$

The distribution function for the photon in environments of extremely high density is the same as that in equation (4.2.1). Therefore, calculation of the finite density corrections to the coupling constant are not as straightforward and require analysis of a dynamical photon mass that stems from corrections to the electric permittivity and magnetic permeability of the region of interest. An effective charge results from correcting these electromagnetic properties, and the corrected coupling constant is calculated by Masood [29] in terms of the chemical potential as

$$\alpha_R = \alpha_0 \left(1 - \frac{2\alpha}{m^2} \left[\frac{\mu^2 - 2m^2}{8} \left(1 - \frac{m^2}{\mu^2}\right) \right] \right) \quad [4.2.9]$$

Equation (4.2.9) is only valid for regions where density effects dominate thermal effects. A reasonable assumption is made that the chemical potential will also be much larger than the mass of the electron, since (4.2.8) suggests that a high chemical potential suppresses QED corrections to the mass. In this limit, the coupling constant can be written in the approximate form as

$$\alpha_R \approx \alpha_0 \left(1 - \frac{2\alpha}{8} \frac{\mu^2}{m^2}\right) \quad [4.2.10]$$

Equations (4.2.4) and (4.2.5) verify that for extremely high temperatures, contributions to mass renormalization and charge renormalization are parameters that cannot be deemed negligible. Circumstances where density effects dominate thermal effects have also been calculated. The negative quadratic relationship will play an important role when considering possible bound states, or density of states, within a certain region under these extreme conditions. These corrections will provide greater insight to the electrodynamic properties and, more specifically, the Lamb shift for environments of extreme temperatures and densities.

Lamb Shift at Finite Temperature

It was determined in section 1 of this chapter that previous results do not allow for the Lamb shift to exist in extreme astronomical environments. These approaches in determining thermal corrections to the Lamb shift involved typical quantum mechanics approaches, and turned out to yield incorrect results for extremely high temperatures. It was shown in section 2 that a relativistic field theory approach is necessary to properly describe the system.

Thermal corrections to the Lamb shift, calculated in section 3, can be made by substituting expressions for the renormalized mass (4.2.4) and coupling constant (4.2.5). Though emphasis will be put on the high temperature limit, the low temperature limit will be briefly discussed to verify the importance of the relativistic field theory approach. In the low temperature limit ($T \ll m$), the Lamb shift is written as

$$\Delta E_{2S\frac{1}{2}-2P\frac{1}{2}} = m_e \left(1 + \frac{\alpha\pi T^2}{3m^2} \right) \frac{\alpha^5}{6\pi} \left[\ln \left(\frac{\Delta E_{2P}}{\alpha^2 \Delta E_{2S}} \right) + \frac{91}{120} \right] \quad [4.3.1]$$

A plot of the Lamb shift as a function of the temperature to mass ratio T/m can be viewed in Figure 4.3. It is important to note here that Knight [7] showed that, due to

blackbody radiation effects, there would be no observable change in the difference in energy between states as temperature increases since individual thermal corrections would shift levels equally in the opposite directions, thereby cancelling thermal effects. However, it is shown here that in the low temperature limit, corrections to the electron mass show that there will be a very small increase in the separation between the energy levels, thereby disagreeing with the results by Knight. Of course, these shifts are extremely small, and only differ from the original Lamb shift value at temperatures near m by approximately 1%.

In the high temperature limit ($T \gg m$), the mass and coupling constant are renormalized, so the Lamb shift is written as

$$\Delta E_{2S\frac{1}{2}-2P\frac{1}{2}} = \frac{m_e \alpha^5}{6\pi} \left(1 + \frac{\alpha \pi T^2}{2m^2}\right) \left(1 + \frac{\alpha^2 T^2}{6m^2}\right)^5$$

$$\times \left[\ln \left(\frac{\Delta E_{2P}}{\alpha^2 \left(1 + \frac{\alpha^2 T^2}{6m^2}\right)^2 \Delta E_{2S}} \right) + \frac{91}{120} \right] \quad [4.3.2]$$

where the coupling constant α and the mass m_e are taken to be the renormalized values corresponding to $T = 0$. The Lamb shift is plotted as a function of the temperature to mass ratio in Figure 4.4. In the high temperature limit, thermal corrections to the mass contribute sizeable increases to the Lamb shift. Thermal corrections to the coupling constant will further contribute to the shift, where these corrections were not present in the low temperature limit. Near the decoupling temperature, thermal corrections account for over 50% of the total Lamb shift, vacuum corrections included. It is clear that thermal contributions at these energies cannot be ignored, as they account for the majority of the shift in energy.

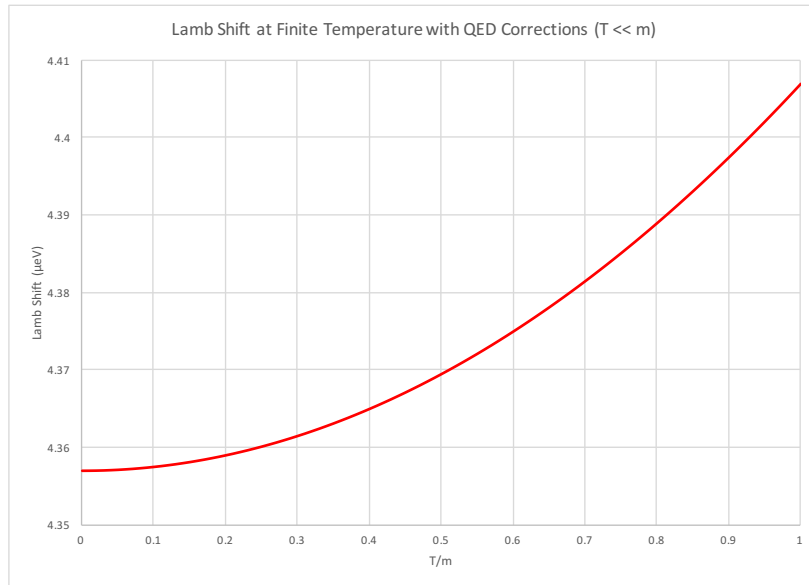


Figure 4.3 – Lamb Shift at Finite Temperature with QED Corrections ($T \ll m$)

A plot of the Lamb shift as a function of the temperature to mass ratio from 0 MeV up to approximately 0.511 MeV. In Kelvin, these temperatures would range from 0 K to approximately 6,000 K.

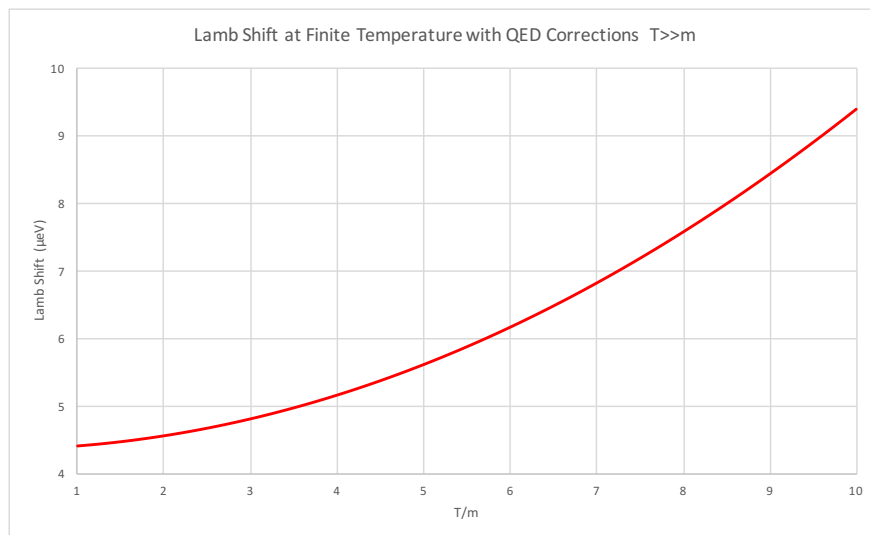


Figure 4.4 – Lamb Shift at Finite Temperature with QED Corrections ($T \gg m$)

A plot of the Lamb shift as a function of the temperature to mass ratio from approximately 0.511 MeV to the predicted decoupling temperature [5] of approximately 5.11 MeV.

In the high temperature limit, thermal corrections to the mass contribute sizeable increases to the Lamb shift. Thermal corrections to the coupling constant will further contribute to the shift, where these corrections were not present in the low temperature limit. For example, from 0.511 MeV to 1.02 MeV, a 4% increase in the Lamb shift is observed. Overall, this is a 5% increase to the Lamb shift calculated with only vacuum radiative corrections taken into account. Near the decoupling temperature, thermal corrections account for over 50% of the total Lamb shift, vacuum corrections included. It is clear that thermal contributions at these energies cannot be ignored, as they account for the majority of the shift in energy.

It is now important to discuss the results of Knight [7] that were determined in the high temperature range. Though the QED results disagree with the assessment that the shift in energy will be identical for all energy states, the mixing between the $2S_{1/2}$ and $2P_{1/2}$ states occurred before Lamb shift calculations were taken into consideration, thereby claiming that the degeneracy between the states is broken before taking QED radiative corrections into account. This shift was given by equation (4.1.7) and plotted in Figure 4.1.

Further corrections to the results given by Knight [7] can be made in recognizing that the constant value of the Lamb shift in (4.1.7) is not constant following the thermal corrections made in this chapter. This leading term will be increasing with increasing temperature as shown in Figure 4.4. The mass and coupling constant are also renormalized to accommodate thermal corrections, so that equation (4.1.7) is more accurately written as equation (4.3.3). In this form, it can be seen that the coupling constant will eventually play a dominant role at extremely high temperatures. It is therefore expected that the continuously increasing function shown in Figure 4.1 is not correct, and the Lamb shift will approach a maximum value.

$$\Delta E_{2S\frac{1}{2}-2P\frac{1}{2}} = \left(\frac{m_e \left(1 + \frac{\alpha\pi T^2}{2m^2}\right) \alpha^5 \left(1 + \frac{\alpha^2 T^2}{6m^2}\right)^5}{6\pi} \left[\ln \left(\frac{\Delta E_{2P}}{\alpha^2 \left(1 + \frac{\alpha^2 T^2}{6m^2}\right)^2 \Delta E_{2S}} \right) + \frac{91}{120} \right] \right) \times \left(1 + \frac{4\pi T^2}{\alpha \left(1 + \frac{\alpha^2 T^2}{6m^2}\right) m^2 \left(1 + \frac{\alpha\pi T^2}{2m^2}\right)^2} \right) \quad [4.3.3]$$

The first parenthetical quantity is the thermally corrected Lamb shift, and the second is Knight's correction from the mixing of the states with thermally corrected mass and coupling constant. A plot of equation (4.3.3) is shown in Figure 4.4 as a function of the temperature to mass ratio.

This correction still gives rather large contributions to the Lamb shift, especially in comparison to (4.3.2). However, if the shift in energy between the states takes place prior to QED corrections, it must be included for the overall thermal correction. As seen in Figure 4.5, the thermal corrections to the charge and mass still play an important role in the overall shift. Up to the decoupling temperature, the Lamb shift calculated here is nearly half the value predicted by Knight. This is due to the increased mass of the electron at high temperatures, as well as the increased coupling constant, insinuating that at high temperatures, the increase in chemical potential is able to overcome the extreme external effects of the surrounding environment, allowing for the bound state to maintain its existence.

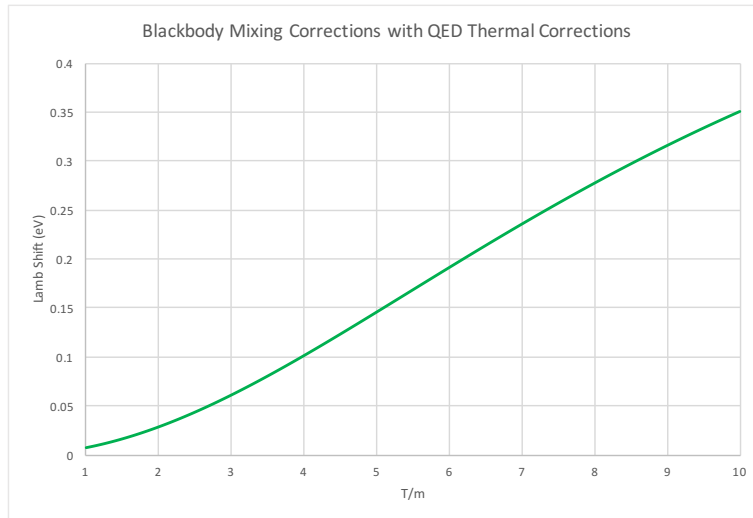


Figure 4.5 – Blackbody Mixing Corrections with QED Thermal Corrections

Masood’s QED thermal corrections are included in Knight’s blackbody radiation corrections for the mixing of the $2S_{1/2}$ and $2P_{1/2}$ states. The Lamb shift with these corrections is plotted up to the decoupling temperature.

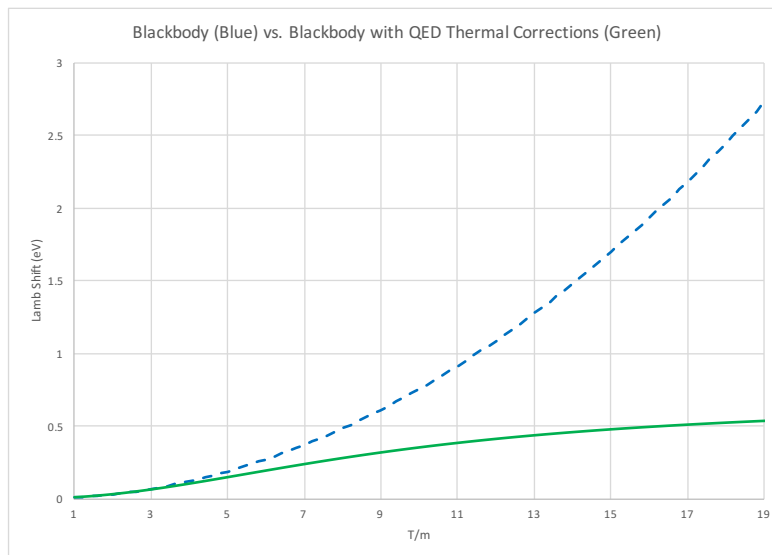


Figure 4.6 – Comparison of Blackbody Corrections and QED Blackbody Corrections

A comparison between Knight’s blackbody radiation corrections (Blue-dashed) and Knight’s corrections with the inclusion of the thermally corrected mass and coupling constant (Green).

As a further extension to note the importance of the renormalized coupling constant at high temperatures, it is recognized that the plot in Figure 4.5 shows a decreasing rate of change in the shift in energy, whereas Figure 4.1 showed a continuously increasing value for the Lamb shift. The two are plotted against one another in Figure 4.6.

Though analysis of the Lamb shift in environments greater than the decoupling temperature require the incorporation of electroweak theory, it may still be interesting to note that thermal corrections to QED still theoretically show asymptotic behavior to the shift in energy between the $2S_{1/2}$ and $2P_{1/2}$ states.

Lamb Shift at Finite Chemical Potential

External thermal contributions in extreme environments have been shown to not allow for bound states. The interior of a Neutron star has extremely high temperature, where these effects by themselves would never allow for bound states. However, stellar cores tend to have extremely high density. The interior of a Neutron star is thought to be so dense that the chemical potential far exceeds temperature effects. In this limit, the Lamb shift has negligible thermal dependency and is corrected only through the chemical potential contributions (4.2.8) and (4.2.10).

$$\Delta E_{2S_{1/2}-2P_{1/2}} = \frac{m_e \alpha^5}{6\pi} \left(1 - \frac{\alpha \mu^2}{\pi m^2}\right) \left(1 - \frac{2\alpha \mu^2}{8 m^2}\right)^5 \left[\ln \left(\frac{\Delta E_{2P}}{\alpha^2 \left(1 - \frac{2\alpha \mu^2}{8 m^2}\right)^2 \Delta E_{2S}} \right) + \frac{91}{120} \right]$$

Figure 4.7 shows that an increasing chemical potential will eventually lead to degeneracy between the $2S_{1/2}$ and $2P_{1/2}$ states that was once broken by vacuum QED corrections. When the chemical potential is at energies around $\mu \sim 10.7$ MeV in comparison to the electron mass, electrons will exist in degenerate energy states which

may give insight to more interesting physical phenomena that is left for discussion in the upcoming section.

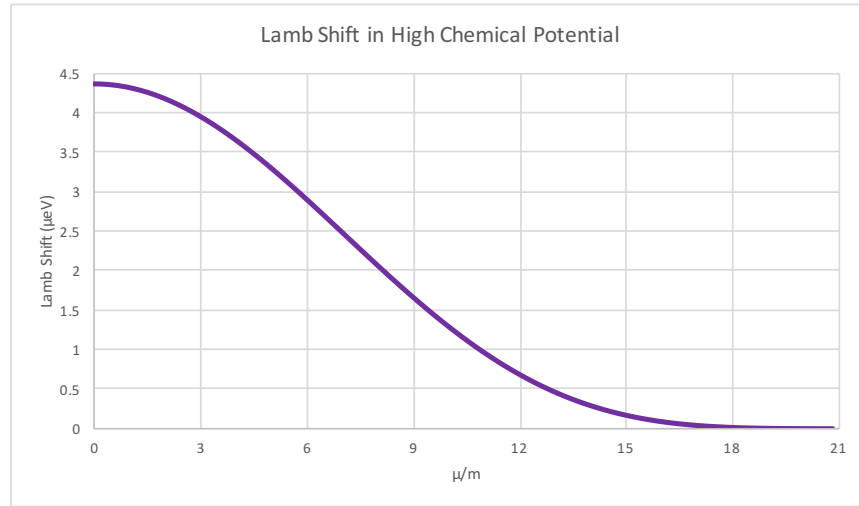


Figure 4.7 – Lamb Shift in High Chemical Potential

A Plot of the Lamb shift in environments where chemical potential contributions are much larger than thermal contributions.

Discussion of Results and Extensions

It is evident from the results in this chapter that in order to properly describe finite temperature and density effects on the Lamb shift, and therefore hydrogen structure, quantum mechanics alone is not sufficient; FTD corrections to QED must be included. At low temperatures, Knight showed using techniques in quantum mechanics that blackbody radiation corrections would not shift energy levels. However, Knight [7] uses only a Bose-Einstein distribution to account for statistical effects in the non-relativistic limit. By using Masood's thermally corrected propagators, it was shown that there will

be contributions to the Lamb shift in the low temperature limit. In the high temperature limit, Knight shows that thermal corrections will shift all states equally, and will therefore not provide any further separation between the $2S_{1/2}$ and $2P_{1/2}$ energy levels. This too was shown to be false by using the thermally corrected propagators. It is interesting to note Knight's value in equation (4.1.5) in that it is identical to Masood's mass correction for the low temperature limit. It may be possible that Knight's high temperature contribution to the overall energy was originally misinterpreted, and this should have been a contribution to the mass. Knight's calculations are still useful as they verify that the electron will not be able to exist in a bound state in these environments, and his inclusion of the mixing is necessary for more accurate calculations of the overall shift. Regardless of the unlikeliness of bound states in these environments, calculation of the Lamb shift with QED thermal corrections is argued to maintain its relevance as it provides insight to the states in which the free electrons may exist relative to one another.

In the high temperature limit, temperatures are in the range of $10^9 \sim 10^{10}$ K. Known astronomical environments where electrons may exist in this temperature range correspond to the interior of Neutron stars. Even though quantum mechanics does not allow for the electron to exist within the nucleus, and Neutron stars are meant to represent large nuclear systems, relativistic electrons are expected to exist in these environments due to the size of the Neutron star. Therefore, Lamb shift corrections are also relevant in this extreme environment. In the interior of the Neutron star, density effects cannot be ignored, and it is possible for chemical potential contributions to exceed thermal contributions to the self-energy of the electron, allowing for possible bound states. In extremely dense environments it is assumed that the mass and coupling constant only need to be renormalized in terms of the chemical potential. An interesting result from this is that a continued increase in chemical potential will even overcome vacuum

contributions to the Lamb shift, ultimately creating degeneracy in the energy states. This could provide very important insight to the structure and formation of Neutron stars and other highly dense environments, such as White Dwarf stars.

At extreme temperatures, relativistic effects cannot be ignored as the threshold energy for electron-positron pair production is exceeded, and these electron-positron pairs will interact statistically with the electron propagator. Therefore, an analysis involving Fermi-Dirac distributions for the electron is necessary. Masood [19, 29] uses a Fermi-Dirac distribution in the renormalization of the fermion propagator to determine renormalized mass and coupling constants. This renormalization scheme is pertinent in order to properly describe the importance that the chemical potential has on the structure and stability of the hydrogen atom in extreme environments, and has been used to improve upon conclusions reached by Knight.

It may also be considered that thermal QED corrections would have an effect on the thermal fluctuations determined by Kolomeisky [10]. However, the range for meaningful contributions proved to be too limited, and otherwise negligible in the high temperature region. Therefore, these results were not further improved upon by including thermal corrections to the mass and coupling constant. In extremely dense environments where bound states may exist, it is assumed that thermal fluctuations will be suppressed by the chemical potential contributions.

Thermal corrections to QED, though reasonably neglected in most calculations, cannot be ignored in extreme environments. Therefore, it is reasonable to believe that there may be other previously neglected factors which also have large contributions in these environments, one of which is extremely high density. Further analysis regarding bound states in a Neutron star should also include magnetic contributions, as magnetic field strengths in this environment are $\sim 10^{12}$ T. This can be done by introducing a

magnetic energy term to the Hamiltonian in equations (4.2.1) and (4.2.2). The external magnetic field will cause different spin states to have different energies. In order to discuss the effects of spin splitting, an addition to the overall energy is given by the Landau energy levels [1] as

$$E = (2n + 1)\hbar\omega_c \pm \frac{1}{2}g\mu_B B \quad [4.4.1]$$

This contribution may be valid for the quantum limit condition $kT < \hbar\omega_c$, where ω_c is the cyclotron frequency for an orbital electron. This limit is achieved in the consideration of strong chemical potential contribution. It should also be noted that since the g -factor depends on the coupling constant, and the cyclotron frequency and Bohr magneton depend on electron mass, a thermally dependent magnetic energy is expected. Landau levels become increasingly more important when discussing density of states, and further analysis may provide the possibility for a quantum hall fluid to exist within extremely dense environments exposed to an extreme magnetic field strength.

QED thermal and density corrections have been shown to be an important dialogue regarding effects on electromagnetic properties, the Lamb shift, and structure of bound states in extreme environments. This has been verified in the low and high temperature limits, as well as high density limits, relative to the electron mass. Though thermal contributions have been shown to not typically allow for bound electrons, insight has been given to how the electron states may exist relative to one another. In extremely dense media, a high chemical potential may allow for bound electrons so long as the condition $\mu \gg T > m$ is valid. It has also been pointed out that the relevant astronomical environments for these effects tend to have strong magnetic fields associated with them. It is expected that further corrections to the Lamb shift can be made by including magnetic field contributions. These are expected to improve upon the results of this

thesis, but are not expected to be necessary where thermal contributions are dominant. Only higher order QED thermal corrections may yield more accurate results in these regions.

REFERENCES

- [1] T. Lancaster and S.J. Blundell. *Quantum field theory: For the gifted amateur*. (2014) New York, NY: Oxford University Press.
- [2] M.D. Schwartz. *Quantum field theory and the standard model*. (2014) New York, NY: Cambridge University Press.
- [3] Zettili, N. *Quantum Mechanics: Concepts and applications*. (2009) West Sussex, United Kingdom: John Wiley & Sons.
- [4] Bransden, B.H., & Joachain, C.J. *Quantum Mechanics* (2nd ed.). (2000) Harlow, England: Prentice Hall.
- [5] Samina Masood. *Renormalization of QED near decoupling temperature*. (2014, June 24) Physics Research International, Article ID 489163, 9 pages. doi:10.1155/2014/489163. Retrieved July 25, 2017, from the arXiv database.
- [6] W.E. Lamb. *Fine structure of the hydrogen atom*. (1955, December 12).
- [7] P.L. Knight. *Effects of external fields on the Lamb shift*. (1972, March) Journal of Physics A: General Physics, 5(3), 417-425. Retrieved July 17, 2017.
- [8] A. Das and B.M. Sidharth. *Revisiting the Lamb shift*. Electronic Journal of Theoretical Physics, 12(34) (2015) 139-152. Retrieved July 25, 2017, from the arXiv database.
- [9] M. Thomson. *Modern Particle Physics*. (2014) Cambridge, United Kingdom: Cambridge University Press.
- [10] E.B. Kolomeisky. *Brownian motion of the electron and the Lamb shift at finite temperature*. (2012, March 6). arXiv database
- [11] T.A. Welton. *Some Observable Effects of the Quantum-Mechanical Fluctuations of the Electromagnetic Field*. (1948, June 4)

- [12] A. Arai. *Derivation of the Lamb shift from an effective Hamiltonian in non-relativistic quantum electrodynamics*. (2014, April) RIMS Kokyuroku Bessatsu, B(45), 1-18. Research Institute for Mathematical Sciences, Kyoto University. Retrieved August 1, 2017, from <http://hdl.handle.net/2433/217421>
- [13] L.D. Landau and E.M. Lifshitz. *Statistical Physics (3rd ed.) Part 1 (Vol 5)*. (1980)
- [14] Samina Masood. *QED at Finite Temperature and Density*. (2012, March 14)
- [15] S. Weinberg. *The Quantum Theory of Fields (Vol 1)*. (1995) New York, NY: Cambridge University Press.
- [16] H. Goldstein, C. Poole, and J. Safko. *Classical Mechanics (3rd ed.)*. (2002)
- [17] Relativistic Quantum Mechanics Lecture Notes. <http://hitoshi.berkeley.edu/221B-S02/Dirac.pdf>
- [18] M.Q. Haseeb and S.S. Masood. *Second Order Thermal Corrections to Electron Wavefunction*. Phys. Lett. B704 (2011) 66-73.
- [19] Samina Masood. *Nucleosynthesis at Finite Temperature and Density*. (2014, March 21)
- [20] G. 't Hooft and M. Veltman. *Regularization and renormalization of gauge fields*. Nucl. Phys. B44 (1972) 189-213.
- [21] A. Weldon. *Covariant calculations at finite temperature: the relativistic plasma*. Phys. Rev. D26 (1982) 1394.
- [22] C. Grupen. *Astroparticle Physics*. (2005)
- [23] J.D. Jackson. *Classical Electrodynamics (3rd ed.)*. (1999)
- [24] R. Kobes and G.W. Semenoff. *Discontinuities of green functions in field theory at finite temperature and density*. Nucl. Phys. B260 (1985) 714; *ibid*, B272 (1986) 239

- [25] E.J. Levinson and D.H. Boal. *Selfenergy corrections to fermions in the presence of a thermal background*. Phys.Rev. D31 (1985) 3280-3284.
- [26] K. Ahmed and Samina Saleem (Masood). *Renormalization and radiative corrections at finite temperature reexamined*. Phys. Rev D35 (1987) 1861.
- [27] K. Ahmed and Samina Saleem (Masood). *Finite-temperature and -density renormalization effects in QED*. Phys. Rev D35 (1987) 4020.
- [28] K. Ahmed and Samina Saleem. *Vacuum polarization at finite temperature and density in QED*. Ann. Phys. 207 (1991) 460.
- [29] Samina S. Masood. *Photon mass in the classical limit of finite temperature and density QED*. Phys. Rev. D44 (1991) 3943.
- [30] Samina S. Masood. *Renormalization of QED in superdense media*. Phys. Rev. D47 (1993) 648-652.
- [31] Mahnaz Haseeb and Samina Masood. *Second order thermal corrections to electron wavefunction*. Phys. Lett. B704 (2011) 66-73.
- [32] Samina Saleem (Masood). *Finite temperature and density effects on electron selfmass and primordial nucleosynthesis*. Phys. Rev. D36, (1987) 2602-2605.
- [33] Samina S. Masood. *Nucleosynthesis in hot dense media*. Astroparticle Physics, 4, (1995) 189.
- [34] R. Kobes. *A Correspondence between imaginary time and real time finite temperature field theory*. Phys. Rev. D42 (1990) 562-572.
- [35] P. Landsman and Ch.G. van Weert. *Real- and imaginary-time field theory at finite temperature and density*. Phys. Rep. 145 (1987) 141-249.
- [36] T. Kinoshita, J. Math. *Mass singularities of Feynman amplitudes*. Phys. 3 (1962) 650-677.

- [37] T. D. Lee and M. Nauenberg. *Degenerate systems and mass singularities*. Phys. Rev. 133 (1964) 1549-1562.
- [38] J. Schwinger. Math. Phys. 2 (1961) 407; J. Schwinger, Lecture Notes of Brandeis University Summer Institute (1960).
- [39] Samina Masood. *Renormalization of QED near decoupling temperature*. Phys. Res. Int. (2014) 48913 (arXiv:1407.1414)
- [40] Tomislav Prokopec, Ola Tornkvist and Richard P. Woodard. *Photon mass from inflation*. Phys. Rev. Lett. 89 (2002) 101301
- [41] V. P. Silin. *On the electromagnetic properties of a relativistic plasma*. Sov. Phys. JETP 38 (1960) 1577.
- [42] Jose F. Nieves and Palash B. Pal. *P- and CP-odd terms in the photon self-energy within a medium*. Phys Rev D39 (1989) 652-659.
- [43] Samina Masood. *Neutrino physics in hot dense media*. Phys.Rev. D48 (1993) 3250.
- [44] S.S. Masood. *Propagation of monochromatic light in a hot and dense medium*. Eur. Phys. J. C77 (2017) 826. <https://doi.org/10.1140/epjc/s10052-017-5398-0> L
- [45] Samina Masood. *Relativistic QED at extremely high temperature*. (2016) arXiv preprint arXiv:1607.00401
- [46] L. Parker. *Particle creation in expanding universe*. Phys. Rev. Lett. 21 (1968) 562
- [47] L. Parker. *Particle creation and particle number in an expanding universe*. J. Phys. A 45 (2012) 374023
- [48] V. N. Tsytovich. *Electromagnetic properties of plasma-like media*. Sov. Phys. JETP, 13(6): (1961) 1775-1787